

**OCEAN RESOURCES INVESTIGATION  
IN THE SEA AREA OF CCOP/SOPAC  
REPORT ON THE JOINT BAFIC STUDY  
FOR THE DEVELOPMENT OF RESOURCES**

**(VOLUME 2)**

**SEA AREA OF COOK ISLANDS**

**February 10, 1987**

**JAPAN INTERNATIONAL COOPERATION AGENCY  
METAL MINING AGENCY OF JAPAN**

M P N
C R (5)
87-17



JICA LIBRARY



1029156[5]

16335



**OCEAN RESOURCES INVESTIGATION  
IN THE SEA AREA OF CCOP/SOPAC  
REPORT ON THE JOINT BAFIC STUDY  
FOR THE DEVELOPMENT OF RESOURCES**

**(VOLUME 2)**

**SEA AREA OF COOK ISLANDS**

**February 10, 1987**

**JAPAN INTERNATIONAL COOPERATION AGENCY  
METAL MINING AGENCY OF JAPAN**

国際協力事業団		
受入 月日	'87. 5. 11	200
登録 No.	16335	661
		MPN



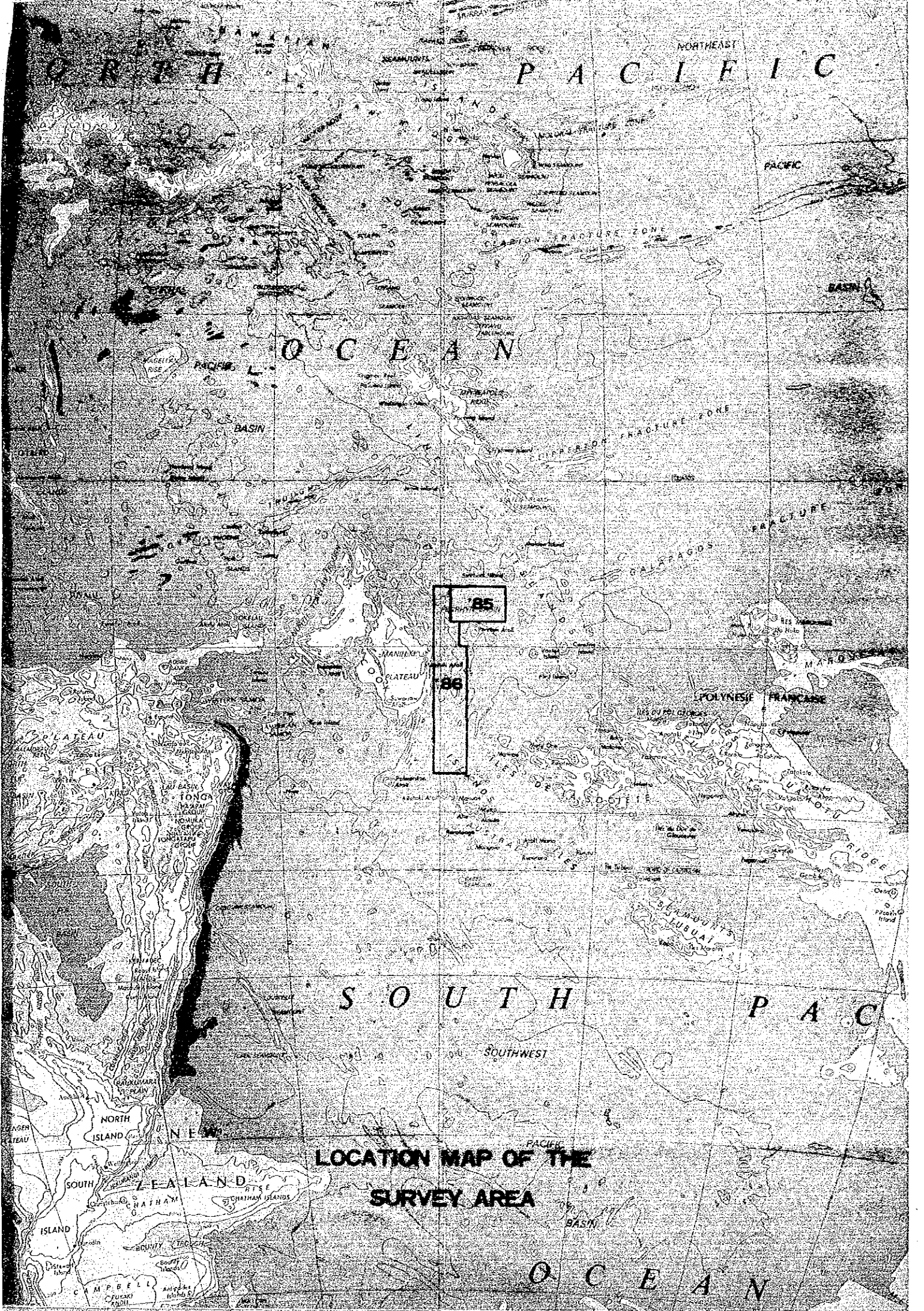
Manganese Nodules in the Surveyed Area: taken by Continuous Deep Sea Camera.  
Diameter of weight is 10 cm.

Upper: Spheloidal manganese nodules. Abundance: 39.8 kg/m<sup>2</sup>. Site number:  
86SFDC0101. Depth: 4,870 m. Location (Latitude: 15°59.68',  
Longitude: 160°00.04')

Lower: Platy manganese nodules. Abundance: 24.2 kg/m<sup>2</sup>. Site number:  
86SFDC0112. Depth: 4,955 m. Location (Latitude: 15°59.78',  
Longitude: 159°38.36')







NORTH PACIFIC OCEAN

OCEAN

SOUTH PACIFIC

LOCATION MAP OF THE SURVEY AREA

OCEAN

85  
86

NEW ZEALAND  
NORTH ISLAND  
SOUTH ISLAND  
HATHAM  
CHRISTIAN ISLANDS  
CAMPBELL

MANILBA  
PLATEAU  
CALPAGOS  
POLYNESIE FRANCAISE  
SUDJETIE  
RIDGE  
BASIN



## PREFACE

In response to the request of the Government of the Cook Islands, Kiribati, and Tuvalu, the Japanese Government decided to conduct a mineral exploration in the South Pacific Offshore Areas, and entrusted the survey to the Japan International Cooperation Agency (JICA) and the Metal Mining Agency of Japan (MMAJ).

For the reason that essential of the above-mentioned survey belong to professional matters, JICA has commissioned practical work to the Deep Ocean Resources Development Co., LTD (DORD).

The survey will be undertaken over a five year period starting from the financial year of 1985. In 1986 the second year, the MMAJ, taking the exclusive economic zone and a adjacent area of the Cook Islands as the sphere of the survey, sent the Hakurei Maru No. 2, a research vessel especially commissioned for prospecting mineral resources on the deep ocean bottom, to the sites of the survey from September 4, 1986 until October 22, 1986, and finished research activities on schedule.

The present report sums up the results of the survey accomplished in the second year.

We hope that this report will serve for the development of the Project and contribute to the promotion of friendly relations between our two countries. We wish to express our deep appreciation to the officials concerned to the Government of above mentioned countries for their close cooperation extended to the team.

February, 1987

Japan International Cooperation Agency

President Keisuke ARITA

Metal Mining Agency of Japan

President Junichiro SATO

## SUMMARY

Pursuant to the request of the Committee for Co-ordination of Joint Prospecting for Mineral resources in South Pacific Offshore Area (CCOP/SOPAC), with a view to confirm the mineral resources potential on the deep ocean bottom along the coast of the Committee's member countries, we continued, this year, the survey in the economic zone and adjacent area of Cook Islands as in the precedent year:

The results of the survey are summarized as follows:

### 1) Outline of the survey

The survey in fiscal year 1986 focussed on the sea areas of approximately 237,700 km<sup>2</sup> delimited by lines 6°30' - 17°30' of south latitude and 158°30' - 160°30' of west longitude, excluding the area accomplished in the last year 1985.

### (1) Methods of the survey

#### 1 Sampling

In the sampling of the manganese nodules and bottom materials, the samplers FG (Free Fall Grab) and SC (Spade Corer) were used. In these cases, the samplers were equipped with a single exposure deep-sea camera in order to observe the sampling points, while samples were taken simultaneously.

#### 2 Observation of the distribution situation of manganese nodules by the continuous deep sea camera (FDC).

#### 3 Echo sounding prospection

In the echo sounding prospection, the following methods were used in combination: PDR (Precision Depth Recorder) to draw up the topographical maps; SBP (Sub-bottom profiler) to measure the acoustic stratigraphy; and (Multi-Frequency Exploration System) to measure the abundance of manganese nodules.

## (2) Survey precision

The primary stage survey was carried out over the whole survey area with the sampling stations' intervals of 42.4 nautical mile grid.

The secondary survey was made in the selected areas where the abundance of manganese nodules was confirmed to be higher by the primary survey, with the sampling stations' intervals of 21.2 nautical mile grid covering the middle points of the samplign stations of the primary survey. During the secondary survey, Sea bottom observation by FDC was also carried out with an interval of 2 nautical miles in a part of the area.

Echo sounding prospection was carried out on the track lines connecting the stations by the shortest distance. Moreover, in case of necessity, supplementary echo soundings were added on the north-south and east-west lines.

## (3) Survey amount

Sampling was executed at 60 stations in total, 20 stations in the primary survey and 40 stations in the secondary survey. The total number of samplings are 180 with 3 samplings at every station.

We get 288 sea-bottom photos by photographing at 51 stations. The mileage covered by the photographing points was about 98.0 miles. Mileage covered by each of the acoustic sounding methods, such as PDR, SBP and MFES etc. was about 4,187 miles.

## 2) Outline of the survey results

### (1) Sea floor topography

Roughly speaking,  $11^{\circ}\text{S}$  latitude makes a border line between the northern part and the southern part having a different situation of sea floor topography and sea floor geology. Sea mounts, sea knolls and hills abound in the northern part. On the contrary the southern part can be said to be flat or quasi-flat from a macroscopic point of view in spite of the sea knoll growth observed in various parts.

The area is deep in general; around 5,200 m deep in the hill area and around 5,500 m - 6,000 m deep in the northern channel areas but has a trend of getting shallower gradually southward from the 11°S latitude and the depth is less than 5,100 m at 11°S - 17°S latitude.

The north-western part of surveyed sea area corresponds to a part of eastern edge of the Manihiki plateau and abound in sea mouths higher than 1,000 m.

(2) Bottom materials

The sea bottom geology is represented by the nature of bottom materials, SBP types and the thickness of echo sounding transparent layer etc. some of them show different aspects between the northern part and the southern part like in the topography. On the whole bottom materials are composed mainly of brown clay and are accompanied by calc-siliceous clay and foraminifera ooze. No remarkable difference is observed between the northern and southern parts. SBP types and the thickness of echo-sounding transparent layer, show apparently the universal development in the southern part rather than the northern part.

CCD (Carbonate compensation depth) estimated by the lowest limit depth of calcareous sediments development is between 5,050 m - 5,150 m and has a slight trend of deepening northwards.

(3) Distributions of the manganese nodules

The manganese nodules in the surveyed sea area bear spheroidal, massive, gravel, ellipsoidal flat, flat-gravel and plate types. Some of them undergo a change into pavement and crust types locally. Almost all of them belong to S-type (smooth type) in the classification by the surface structure.

The abundance of manganese nodules is extremely of high value being 17.14 kg/m<sup>2</sup> in average and 34.5 kg/m<sup>2</sup> in maximum of the 60 survey points. General tendency of abundance is low in the northern part and high in the southern part. The areas having particularly high value are following 2 areas.

- (i) 10°S - 11°S: area of about 6,200 km<sup>2</sup>, average abundance of 20.53 kg/m<sup>2</sup>, maximum abundance of 34.11 kg/m<sup>2</sup>
- (ii) 15°S - 16°30'S: area of about 12,300 km<sup>2</sup>, average abundance of 24.68 kg/m<sup>2</sup>, maximum abundance of 34.57 kg/m<sup>2</sup>

3) Grade and metal contents distributions of manganese nodules

The grade of manganese nodules in the sea area surveyed this year is characterised by high Co and low Ni and Cu content. Especially Co grade exceeds 0.4% in the 69% of sampling points, 0.5% in the 31% of them and reaches a maximum value of 0.61%. The grade distribution has the same tendency of change in the direction of south to north as the nodule abundance. That is to say that the abundance of Co grade and generally high in the southern part, and Ni grade and Cu grade are high in the northern part. Fe grade like Co grade is high in the southern part and Mn grade like Ni grade and Cu grade is high in the northern part. The metal grade distribution is high throughout the area under the influence of manganese nodules abundance which is high throughout the area. As for the Co content, it is apparent that it shows a higher value in the southern part.

Table shows the comparison of the high abundance of manganese nodules in the area surveyed this year with the abundance observed last year. Incidentally, the distribution area with a Co metal content of more than 20 g/m<sup>2</sup> are 22 times larger than last year's distribution areas.

Comparison of metal contents distribution

	Survey area 1985		Survey area 1986	
	Distribution area (km <sup>2</sup> )	Average metal content (g/m <sup>2</sup> )	Distribution area (km <sup>2</sup> )	Average metal content (g/m <sup>2</sup> )
Ni	7,500	29.2	96,270	38.4
Cu	630	23.2	41,590	27.0
Co	4,700	31.5	102,140	74.7

## CONTENT

Chapter 1. Forward .....	1
Chapter 2. Main Points of the Survey .....	2
2-1 Title of the Survey .....	2
2-2 Sea Areas of the Survey .....	2
2-3 Objectives of the Survey .....	2
2-4 Period of the Survey .....	
2-5 Participants in the Survey .....	3
2-6 Apparatus and Equipment Used in the Survey .....	4
1) Vessel positioning system .....	4
2) Echo sounder .....	4
3) Exploring equipment for mineral resources in deep-sea beds .....	4
4) Sampling apparatus .....	5
5) Assaying equipment .....	5
6) Data processing system .....	5
Chapter 3. Methods of the Survey .....	6
3-1 Numbering of the Track Lines, Sampling Stations and Sampling Points .....	6
1) Numbering of the track lines .....	6
2) Numbering of the sampling stations and sampling points .....	6
3-2 Vessel Positioning .....	9
3-3 Survey of the Sea Floor Topography .....	10
3-4 Survey on the Superficial Sediments .....	10
3-5 Research on Manganese Nodules by Means of MFES .....	11
3-6 Sampling by Means of FG and SC, and Sea bottom Observation by Means of Deep-Sea Camera .....	11
1) Sampling by FG .....	11
2) Sampling by SC .....	13
3) Sea bottom observation by deep-sea camera .....	13
4) Evaluation of the grab operations by FG sampler and of sample collection accuracy .....	14
3-7 Processing, Analyzing and Storing of Samples .....	14



3-8	Sea Bottom Observation by Means of FDC	19
	1) Selection of the track lines for FDC	19
	2) Interval of observation stations of FDC	19
	3) Number of photos by FDC	21
	4) Photographing operations of FDC	21
	5) Analysis of the photos by FDC	21
3-9	Processing and Analyzing of the Survey Data	23
	1) Surveying data and their processing	23
	2) Analyzing of the survey data	24
Chapter 4. Results of the Survey		27
4-1	Survey Achievements	27
4-2	Sea Floor Topography	29
4-3	Superficial Sediment	35
	1) Classification of SBP records	35
	2) Distribution of SBP types	40
	3) Thickness and its distribution of upper transparent layer in SBP profiles	41
4-4	Research on Manganese nodules by means of MFES	42
	1) Factors affecting on MFES	42
	2) Estimation of manganese nodules by means of MFES	49
4-5	Bottom Materials	52
	1) Distribution of bottom materials	52
	2) Classification of bottom materials	55
	3) Properties of bottom materials	55
	4) Composing minerals of bottom materials	57
	5) Chemical composition of bottom materials	60
	6) Authigenic minerals of bottom materials	62
	7) CCD	63
	8) Identification of microfossils in bottom materials	63
4-6	Sea Bottom Observation	82
	1) Observation by FDC	82
	2) Observation by deep-sea camera	92
	3) Comparison with the results of FG sampling	92

4-7	Assaying	95
	1) Inspection on the bias	95
	2) Examination of the results	96
4-8	Manganese nodules	98
	1) Physical properties (morphology and granular size-characteristics by external appearance)	98
	2) Chemical properties (5 principal components-total analysis-micro-analysis-chemical properties of section)	104
	3) Mineral properties	123
	4) Distributional characteristics of manganese nodules	132
	(1) Morphology distribution of manganese nodules	132
	(2) Size distribution of manganese nodules	132
	(3) Granular size and morphology	132
	(4) Topography and morphology	132
	(5) SBP types and morphology	136
	(6) Bottom materials and morphology	136
	5) Sea bottom situation and abundance	141
	(1) Morphology and abundance of the manganese nodules	141
	(2) Sea floor topography and abundance	141
	(3) SBP type and abundance	146
	(4) Upper transparent layers and abundance	146
	(5) Bottom materials and abundance	146
4-9	Bearing Situation of Manganese Nodules	149
	1) Abundance of the manganese nodules	149
	2) Grade distribution	149
	3) Distribution of metal content (Ni, Cu, Co)	150
	4) Geological factors and abundance of manganese nodules	153
Chapter 5. Summary		156
	1) Water depth, sea bottom topography and geology.	156
	2) Characteristic features of manganese nodules.	156
	3) Abundance, grade and metal contents distribution of manganese nodules.	157

### List of inserted tables

Table 4-1-1	List of Survey Achievements	27
Table 4-2-1	Classification of Sea Floor Topography	30
Table 4-5-1	Sampling Ratio of Bottom Materials	52
Table 4-5-2	Classification Criteria of Bottom Materials	55
Table 4-5-3	Results of X-ray Diffraction Analysis of Bottom Materials	58
Table 4-5-4	Chemical Composition of the Bottom Materials	61
Table 4-5-5	Mutual Relations among Metal Content in the Bottom Materials	62
Table 4-5-6	List of the Collected Radiolarias	65
Table 4-5-7	List of the Collected Foraminifera	73
Table 4-5-8	Summary of Geological Environmental Analysis Based on Fossiles in the Bottom Materials	80
Table 4-6-1	Coverage and Abundance of Manganese Nodules at Each Stations of FDC-Survey	83
Table 4-6-2	Comparison of Abundances Obtained by FG Sampling and FDC Survey	94
Table 4-7-1	Estimated Values of a, b and Correlation Coefficients	97
Table 4-7-2	Examination of the Bias and the Accidental Errors by Regression Analysis	97
Table 4-7-3	Bias and Accidental Errors Resulting from Inspection of the Difference of Average Values	97
Table 4-8-1	Physical Properties Associated with Morphology of Manganese Nodules	101
Table 4-8-2	Chemical Properties of Manganese Nodules	108
Table 4-8-3	Morphology and Chemical Properties of Manganese Nodules	110
Table 4-8-4	Size and Chemical Properties of Manganese Nodules	111
Table 4-8-5	Sea Floor Topography and Chemical Properties of Manganese Nodules	112
Table 4-8-6	Bottom Sediments and Chemical Properties of Manganese Nodules	114
Table 4-8-7	Chemical Composition of Manganese Nodules	115
Table 4-8-8	Chemical Compositional Difference Between Surface and Inner Part Nodules	119
Table 4-8-9	Results of EPMA Analysis of the Manganese Nodules	121
Table 4-8-10	Results of X-ray Diffraction Analysis of the Manganese Nodules	125

Table 4-8-11	Relation Between Regional Sea Floor Topography and Abundance of Manganese Nodules	144
Table 4-8-12	Relation Between Local Sea Floor Topography and Abundance of Manganese Nodules	145
Table 4-9-1	High Abundance Zone of Manganese Nodules	150
Table 4-9-2	Comparison of the Results between 1985 and 1986	152

List of the inserted figures

Colour:	Representative Occurrences of Manganese Nodules	
	Location Map of the Survey Areas	
Figure 3-1-1	Explanation of Numbering of Stations and Sampling Points	7
Figure 3-1-2	Numbering of the Areas in the Surveyed Sites	8
Figure 3-6-1	Distribution Density of Sampling Stations	12
Figure 3-6-2	Explanation on the Setting Order of Three Samplers at a Sampling Station	13
Figure 3-6-3	Calculating Criteria of Grab Precision	14
Figure 3-7-1	Processing and Assaying Flowsheet of Samples (No. 1 and 2)	16
Figure 3-7-2	Acoustic Sounding and Processing Flowsheet	18
Figure 3-8-1	Track Lines and Observation Stations of FDC-Survey	20
Figure 4-2-1	Explanation of Sea Floor Topography	31
Figure 4-2-2	Section of Sea Floor Topography	33
Figure 4-3-1	Classification of SBP Records (No. 1, 2 and 3)	37
Figure 4-4-1	Distribution of Weight Coefficient	44
Figure 4-4-2	Relation Between MFES Intensity and Abundance of Manganese Nodules (No. 1, 2 and 3)	46
Figure 4-4-3	Distribution of Embedded Type Manganese Nodules	48
Figure 4-4-4	Influence of Embedded Type Manganese Nodules on MFES Measurement	51
Figure 4-5-1	Distribution of Bottom Materials	53
Figure 4-5-2	Smear Slide Photos of Bottom Sediments	56
Figure 4-5-3	Typical Pattern of the X-ray Diffraction of Bottom Sediment	59
Figure 4-5-4	Variation Diagram of CCD (Carbonate Compensation Depth) in the Surveyed Area	63
Figure 4-5-5	Microscopic Photos of Bottom Sediment	66

Figure 4-5-6	Species of the Typical Radiolarian Fossil (No. 1 and 2)	67
Figure 4-5-7	Species of the Typical Foraminifera Fossil (No. 1 and 2)	74
Figure 4-6-1	Modified Occurrence of Manganese Nodules Obtained by FDC Survey	85
Figure 4-6-2	Examples of Continuous Photos by FDC	87
Figure 4-6-3	Examples of Photos by FDC	89
Figure 4-6-4	Examples of Deep-Sea Bottom Photos and of Re-collected Photos	93
Figure 4-8-1	Morphology of Manganese Nodules (No. 1 and 2)	99
Figure 4-8-2	Morphology, Size and Sampling Weight of Manganese Nodules	103
Figure 4-8-3	Frequency Distribution of 5 Principal Components	105
Figure 4-8-4	Scatter Diagram Among Respective Components	106
Figure 4-8-5	Relation Between Major Components and Water Depth.	107
Figure 4-8-6	Photos of Manganese Nodules Used for Section Analysis	117
Figure 4-8-7	Photos of Manganese Nodules used for EPMA Analysis	118
Figure 4-8-8	Grade of Respective Section of Manganese Nodules (On Board Analysis)	120
Figure 4-8-9	Grade of Respective Section of Manganese Nodules (EPMA Analysis)	122
Figure 4-8-10	Photos of Manganese Nodules Used for X-ray Diffraction Analysis	124
Figure 4-8-11	X-ray Diffraction Pattern of the Manganese Nodules (No. 1 and 2)	126
Figure 4-8-12	Macro-Photo and Microscopic Photos of Polished Thin Section of Manganese Nodules (No. 1 and 2)	129
Figure 4-8-13	Morphology Distribution of Manganese Nodules	133
Figure 4-8-14	Size Distribution of Manganese Nodules	133
Figure 4-8-15	Relation Between Size and Morphology	135
Figure 4-8-16	Relation Between Local Topography and Morphology	137
Figure 4-8-17	Relation Between SBP Type and Morphology	138
Figure 4-8-18	Relation Between Upper Transparent Layer Thickness and Morphology	139
Figure 4-8-19	Relation Between Bottom Sediments and Morphology	140
Figure 4-8-20	Average Abundance by Respective Morphology and Occurrence Ratio by Respective Abundance of Manganese Nodules	143

Figure 4-8-21 Relation Between SBP Type and Abundance of Manganese Nodules .....	147
Figure 4-8-22 Relation Between Upper Transparent Layer Thickness and Abundance of Manganese Nodules .....	147
Figure 4-8-23 Average Abundance by Respective Bottom Sediments and Occurrence Ratio by Respective Abundance of Manganese Nodules .....	148
Figure 4-9-1 Correlation Diagram among Geological Factors and Characteristic Features of Manganese Nodules .....	155

List of the Annexed Figures

Annexed Figure 1	Tracklines Map .....	174
Annexed Figure 2	Positionsof Sampling Points .....	175
Annexed Figure 3	Sea Floor Topography .....	176
Annexed Figure 4	Distribution Map of SBP Types .....	177
Annexed Figure 5	Acoustic Thickness of UpperTransparent Layers by SBP ..	178
Annexed Figure 6	Estimated Abundance of Manganese Nodules by MFES Intensity .....	179
Annexed Figure 7	Abundance Map of Manganese Nodules .....	180
Annexed Figure 8	Ni Grade Map of Manganese Nodules .....	181
Annexed Figure 9	Cu Grade Map of Manganese Nodules .....	182
Annexed Figure 10	Co Grade Map of Manganese Nodules .....	183
Annexed Figure 11	Mn Grade Map of Manganese Nodules .....	184
Annexed Figure 12	Fe Grade Map of Manganese Nodules .....	185
Annexed Figure 13	Ni Metal Quantity Map .....	186
Annexed Figure 14	Cu Metal Quantity Map .....	187
Annexed Figure 15	Co Metal Quantity Map .....	188

List of the Survey Results

Annexed Documents Wind Direction  
Wind Velocity  
Atmospheric Pressure  
Swell Cycle  
Cloudness  
etc.





## Chapter 1. Forward

In response to the request of the Committee for Co-ordination of Joint Prospecting for Mineral Resources in South Pacific Offshore Areas, we have executed the survey to confirm the deep-sea mineral resources potential in the economic zone of the Cook Islands, using the research vessel "Hakurei Maru No. 2" especially commissioned to explore mineral resources on the deep-sea beds and having technical experience and equipment in studying the field of the manganese nodules.

Thanks to good weather, the survey proceeded satisfactorily and were accomplished on schedule.

The details of the survey are as follows.

## Chapter 2. Main Points of the Survey

### 2-1 Title of the Survey

Deep Ocean Mineral Resources Investigation  
In the Sea Areas of CCOP/SOPAC  
Joint Basic Study for the Development of Mineral Resources in the  
Exclusive Economic Zone of Cook Islands.

### 2-2 Sea Areas of the Survey (cf. Location Map)

Pursuant to the Cooperative Study Programme and its Scope of Work relating to the deep-sea bottom mineral resources in the economic sea areas of CCOP/SOPAC, concluded in July 18, 1986 between the Government of Japan of one part and the Secretariat of CCOP/SOPAC of the other part, the sea areas contained in a polygon (surface: approximately 237,700 km<sup>2</sup>) enclosed by geodesic lines drawn between coordinates numbered in the series listed below were designated as the survey areas.

	Latitude	Longitude
1	6°30'	160°30'
2	6°30'	159°30'
3	8°30'	159°30'
4	8°30'	159°00'
5	10°00'	159°00'
6	10°00'	158°30'
7	17°30'	158°30'
8	17°30'	160°30'
1	6°30'	160°30'

### 2-3 Objectives of the Survey

The objectives of the present survey consisted of confirming the bearing situation of mineral resources distributed over on the deep sea bottom of the Cook Islands sea areas and of other related studies.

## 2-4 Period of the Survey

Survey: September 4, 1986 - October 22, 1986

Analysis: October 23, 1986 - February 10, 1987

## 2-5 Participants in the Survey

### Japanese side

#### Negotiators for the agreement

Fumihiko KIMURA (Ministry of International Trade and Industry)

Toshio SAKASEGAWA (Metal Mining Agency of Japan)

Yoshiyuki KITA ( idem )

#### Supervisors at the surveying sites

Makoto ISHIDA (Metal Mining Agency of Japan)

Seizo NAKAO (Geological Survey of Japan)

Yoshiyuki KITA (Metal Mining Agency of Japan)

#### Members of the surveying team

##### Chief of the team

Motohide HIROTA (Deep Ocean Resources Development: DORD)

##### Member of the team

Toshio TAKAHASHI ( idem )

Hiroshi KUSAKA ( idem )

Kenji KONAGAI ( idem )

Masami HAMANO ( idem )

Kiyoshi TONO ( idem )

Kazunori MATSUI ( idem )

Hisanori TAKAHASHI ( idem )

Kenji SHINOHARA ( idem )

Hiromitsu SHIMOGAMA ( idem )

Koichi HISATANI ( idem )

Nobuyuki MURAYAMA ( idem )

Katsuhiko EBISUI ( idem )

Ichiro YAMASHITA ( idem )

Masatoshi SHINMYO ( idem )

Consigning side

Negotiators for the agreement

Jioji KOTOBALAVU (CCOP/SOPAC)  
C.A. MATOS ( idem )  
D.L. TIFFIN ( idem )

Advisor

D. S. Cronan (CCOP/SOPAC)

Surveying trainee

Vaitoti TUPA (Cook Islands)

**2-6 Apparatus and Equipment used in the Survey**

The main apparatus and equipment used in the survey during the current fiscal year were as follows:

- 1) Vessel positioning system
  - (1) Navy navigation satellite system (NNSS); manufactured by MAGNAVOX
- 2) Echo sounder
  - (1) Precision depth recorder (PDR), 12 kHz; manufactured by NEC
  - (2) Sub-bottom profiler (SBP), 3.5 kHz; manufactured by NEC
  - (3) Narrow beam sounder (NBS), 30 kHz; manufactured by Honeywell ELAC
- 3) Exploring equipment for mineral resources in the deep-sea beds
  - (1) Multi-frequency exploration system (MFES); manufactured by Sumitomo Metal Mining
  - (2) Continuous deep-sea camera system with a finder (FDC); manufactured by DORD
  - (3) Deep-sea camera; manufactured by Preussag

4) Sampling apparatus

(1) Suspended-type sampler

Spade corer (SC); manufactured by Ocean Instruments

(2) Automatic sinking and re-floating type sampler

Free fall grab (FG); manufactured by Preussag

(3) Mud collector for the free fall grab; manufactured by DOMA

5) Assaying equipment

(1) Preparatory treatment equipment (drying, grinding); manufactured by Yoshida Seisakusho.

(2) Fluorescent X-ray analysis equipment; manufactured by Rigaku Denki

6) Data processing system

(1) Data processing system; manufactured by NEC

## Chapter 3. Methods of the Survey

### 3-1 Numbering of the track lines, sampling stations and sampling points

#### 1) Numbering of the track lines

- (1) Numbering was put on the track lines for acoustic sounding, so that the date and order of working were able to be identified by every crusing unit; for instance, 86S0927A, 86S0927B.

For the night crusing, "N" was added to the end of numbers such as 86S0927N.

For the lines merely between sampling points, "P"(Position) was added such as 86S0927P.

In these cases, "86S" means the financial year of the survey (1986) and the study organization (CCOP/SOPAC-S); "0927" indicates the month of September and the date of 27th, and "A, B" the order of measuring lines on that day.

- (2) Measuring lines for FDC (Continuous deep-sea camera with a Finder)

The measuring lines are identified by additional numbers such as 86SCDC01, 86SCDC02 .....

#### 2) Numbering of the sampling stations and sampling points

- (1) In the current financial year, "86S" was prefixed to indicate the financial year of the survey (1986) and the study organization (CCOP/SOPAC-S).
- (2) The surveyed sea area was divided in quadrilaterals formed with the longitudinal and latitudinal lines marked at every  $1^{\circ}$  starting from the origin  $1^{\circ}\text{N}$ :  $175^{\circ}\text{E}$  towards east and south.
- (3) To these quardilaterals the areas numbers were designated as shown in the Fig. 3-1-1.

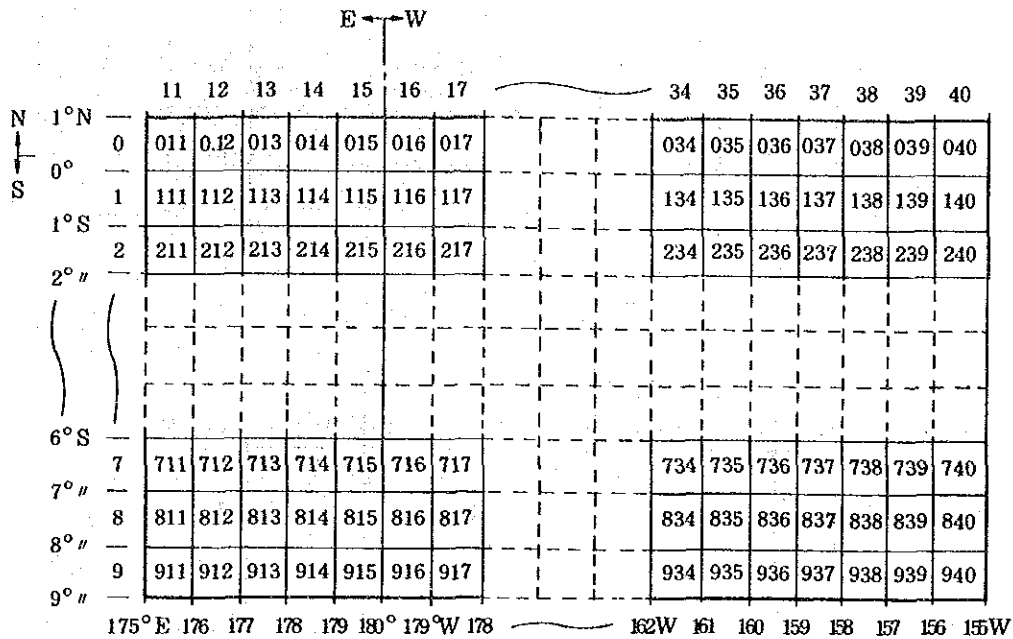


Fig. 3-1-1 Explanation of Numbering of Stations and Sampling Points

That is to say, as the Figure shows, the area of north-west extremity was numbered as "011"; and at every advance eastwards, the number progresses such as 012, 013 .... likewise, at every advance southwards such as 111, 211, 311 .... . Concretely speaking, the figures at the hundred level designate areas in the same latitudinal zone, the figures at the ten level and the one level indicate areas in the same longitudinal zone.

- (4) The areas numbers defined in the previous paragraph (3) correspond to the fourth quadrant of rectangular co-ordinates, the origin of which is at the north-west extremity; in other words, these areas contain north and west sides of the numbered area and not east and south sides.
- (5) The areas surveyed in the current financial year are shown in 2-2 they spread over the south side of the sphere showed in Fig. 3-1-1. The area numberes are as shown in the Fig. 3-1-2.

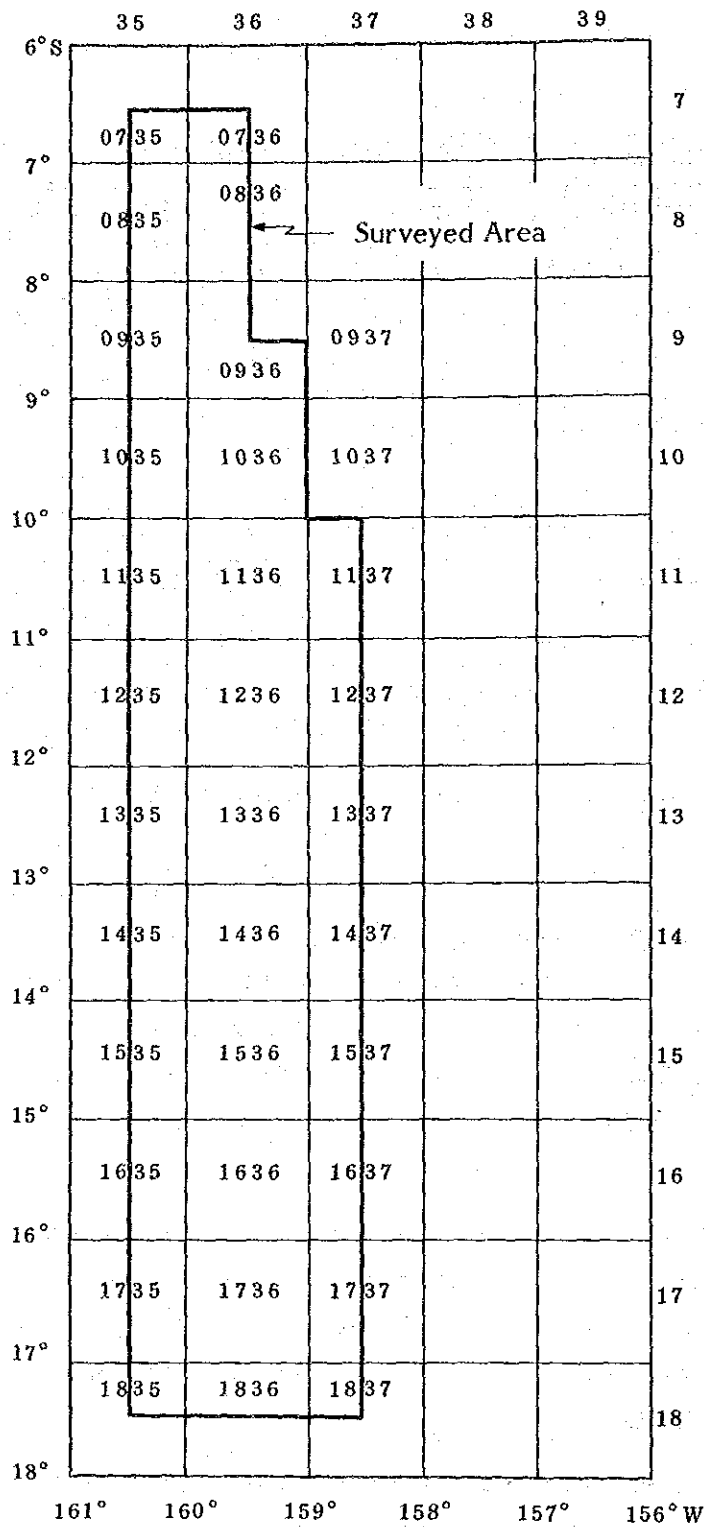


Fig. 3-1-2 Numbering of the Areas in the Surveyed Sites



- (6) The sampling that took place in the areas appointed in the previous paragraph (5) and the samples thus collected were numbered with additional figures beginning from "01", after being marked with signs according to the respective sampling methods. From the numbering point of view, the primary survey and the secondary survey were not distinguished.

FG: samples taken by means of the free fall grab

SC: samples taken by means of the spade corer

- (7) Summing up the above-mentioned explanations, the sample number "86S0836FG01" signifies the 1st sample collected by means of FG in the area 0836, CCOP/SOPAC in 1986.

### 3-2 Vessel Positioning

During the survey, all the vessel positions were indicated by "NNSS". The vessel positions determined by the dead reckoning navigation system during the time elapsed from a certain "UP-DATE"\*1 to the next "UP-DATE", were corrected by proportional allotment according to this time elapsed; namely, the so-called "corrected positions" were adopted.

The vessel positions as follows were registered in the field notes or in other ways to be utilized for the data processing and analysis to be explained later.

- 1 starting and terminating positions on the measuring lines, course alternation points of vessel, positions at every hour of integral number;
- 2 samplers' setting positions and their re-collecting positions;

---

\*1 The "UP-DATE" means the moment of determining vessel position 17 minutes after FIX moment of vessel position given by the satellite. (This determined position is a presumed one) During the survey, 4 satellites were available.

- 3 setting and re-collecting positions of the towing apparatus for observation by FDC, starting and terminating positions of the observation.

All the vessel positions relating to the survey activities were registered in MT with on-line by using the data processing system on board. Also, the corrected vessel positions were printed out by the same system once every minute according to the respective UP-DATE in order to be utilized for filling and analyzing the survey data.

### **3-3 Survey of the Sea Floor Topography**

As for the survey of the sea floor topography, fathoming and topographical observation were practiced mainly by means of PDR between the respective stations and between the respective sampling points. Moreover, on the occasion of observation by FDC, research on the sea bottom topography was carried out in the surrounding areas as well as along the track lines.

Fathoming was carried out every 12 seconds; fathoming values indicated by PDR digitizer were registered on MT with the on-line system.

In addition, every 5 minutes, sea depths were recorded by the registered papers of the PDR and with this data, the sea floor topographic map and other documents were produced.

The survey between the measurement stations was executed generally at the vessel speed of 10 knots, but according to the surveying situation, the vessel speed was accordingly increased or reduced. As for the track lines between sampling points, the vessel speed varied from 3 to 8 knots according to the sampling operation.

### **3-4 Survey on the Superficial Sediment**

The survey of the superficial sediment of the sea bottom was carried out simultaneously with the sea bed survey, by means of SBP (frequency of 3.5 kHz) on all the cruised track lines.

The basic data of the superficial sediment consist of informations such as thickness of transparent layers composing the upper moststratum ont he basis of

the registered section pattern of SBP and acoustic stratigraphy type, etc. This information was marked in their field notes every 10 minutes and used to draw up the contour map of the superficial sediment thickness and SBP type distribution map.

### **3-5 Research on Manganese Nodules by means of MFES**

The survey on the bearing situation of manganese nodules by means of MFES was carried out simultaneously with the research on the sea floor topography and the superficial sediment.

The measuring values of MFES were continuously indicated every 48 seconds by calculating data produced by NBS, PDR and SBP, but the moving average of 15 measured values was taken as MFES values of evidence.

The measuring values of MFES were registered in MT by means of an interface with the data processing system and also these basic data as registered on the MFES floppy-discs about every 5 minutes.

### **3-6 Sampling by means of FG and SC, and Sea bottom observation by means of Deep Sea Camera**

#### **1) Sampling by FG**

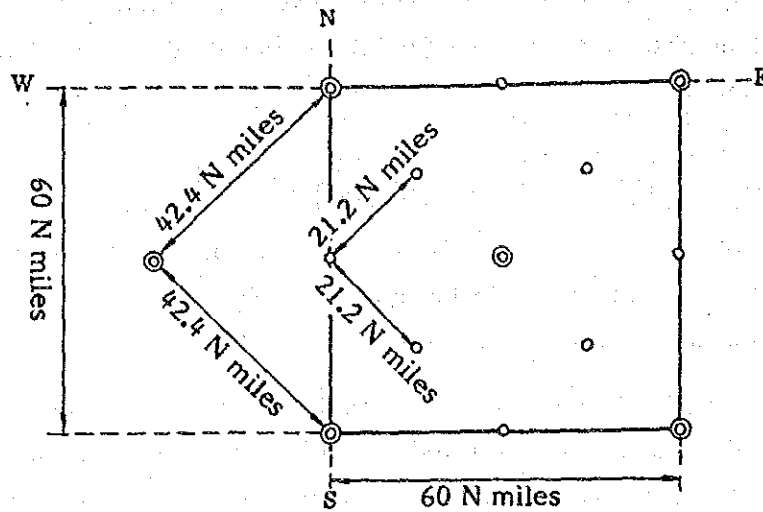
The fundamental chart used for the survey was marked by the sectioning datum lines at every  $1^{\circ}$  (60 miles) in latitude and longitude.

As the sampling operations were based upon this chart, the precision of surveying stations for the primary and secondary surveys were chosen as described as follows:

**Primary stage:** Stations for sampling were fixed on a 42.4 N mile grid connecting the crossing point of sectioning lines at every  $1^{\circ}$  (60 miles) in latitude and longitude to the centre of the section;

**Secondary stage:** Stations covering the middle stations of the primary stage were added and the sampling point interval was reduced to a 21.2 N mile grid.

The above-mentioned scheme is shown in Fig. 3-6-1.



- ⊙ Primary survey station: 42.4 N mile grid
- Secondary survey station: 21.2 N mile grid

- Notes
- 1) 60 N miles section correspond to every  $1^{\circ}$  in latitude and longitude
  - 2) 1 N mile equals to 1.852 km

Fig. 3.6.1 Distribution Density of Sampling Stations

At every surveying station, three samplings were taken and the process is as follows:

The samplers were set down at each apex of the right isosceles triangle the southern apex of which should be located on the given station; the setting down points were considered as sampling points. In other words, sampling was done at every surveying station and then at the two other points respectively 1.4 N miles to the northwest and to the northeast from the station.

From whichever direction the vessel approached the sampling station, it passed through the station once and after confirming the station, it returned to it and set down the first sampler. The setting order in the 3 point sampling system is illustrated in Fig. 3-6-2.

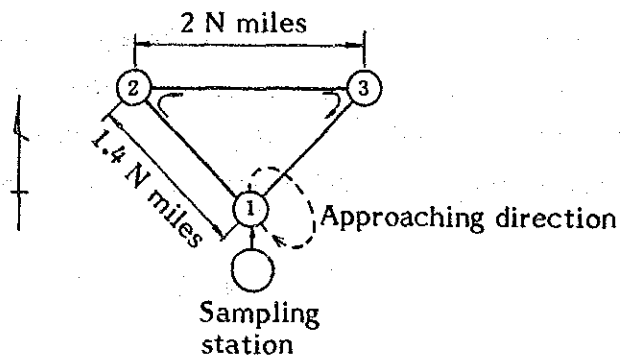


Fig. 3-6-2 Explanation of the Setting Order of Three Samplers at a Sampling Station

### 2) Sampling by SC

In case of using SC instead of FG the sampler is set down, in principle, at the first point among the 3 sampling points. In this case, as in the sampling by FG, the vessel passes the station (1) once and sets down the FG at the stations 2 and 3 of the figure and returns to the sampling station to set down the SC.

The collection of FG is carried out after the SC is collected.

### 3) Sea bottom observation by Deep sea camera

In addition to the sampling by means of FG and SC, one frame photographs of the sea floor were taken by means of deep sea camera attached to each equipment. These photos are used for the purpose of siezing the sea floor situation and supplementing the sampling data. Correction of the abundance of manganese nodules obtained by samplings will also be possible by accumulating the data.

#### 4) Evaluation of the Grab Operations by FG Sampler and of the Sample Collecting Accuracy

In some cases, it can be assumed that the sampling has been insufficient because of the FG grab troubles such as net damage, teeth-breaking and incomplete operation, rare as they may be. (cf. Fig. 3-6-3)

When these cases were ascertained, the covering surface ratio (a) of the manganese nodules seen in the sea bottom photo and the recollecting surface ratio (b) calculated on sample collected, were used to rank the operating accuracy in 4 categories, as shown in Fig. 3-6-3. These categories served as a reference to calculate the abundance.

		a (%)				
		0	5	10	20	100
b/a	> 1.0 0	1	1	1	1	
	1.0 0	1	1	1	1	
	0.7 5	1	2	2	2	
	0.5 0	1	2	3	3	
	0.2 5	1	2	3	4	
	0.0 0					

- |                                  |                                   |
|----------------------------------|-----------------------------------|
| 1. (Collection) complete         | a: Coverage (deep sea camera)     |
| 2. (Collection) fairly completed | b: Coverage                       |
| 3. (Collection) incomplete       | (calculated on samples collected) |
| 4. (Collection) failure          |                                   |

Fig. 3-6-3 Calculation Criteria of Grab Precision

### 3-7 Processing, Analyzing and Storing of Samples

The re-collected samples (manganese nodules and bottom materials) underwent various treatments such various measurements, Fluorescent X-ray analysis etc. on board on the basis of the processing and analyzing flowsheet of

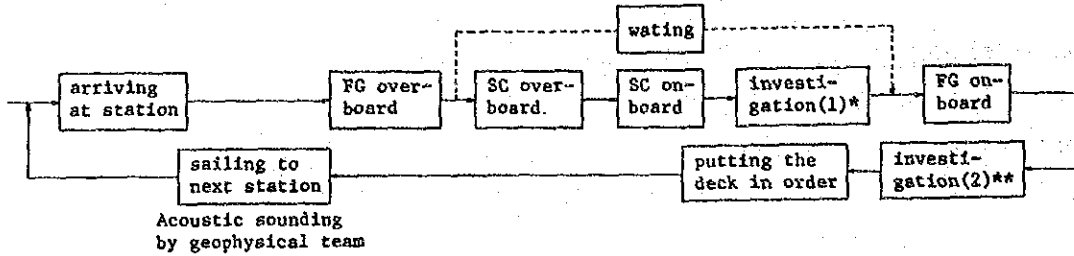
samples by FG and SC shown in the Fig. 3-7-1, also, a part of the samples were taken to the laboratory to be processed for microscopic observation, X-ray diffraction, complete analysis, micro-analysis, etc., and the rest were kept in storage.

SUMMARY OF THE EXPLORATION WORK ON BOARD

The exploration work is carried out by the geological team and geophysical team respectively. The main works of our exploration are the bottom sampling and the acoustic sounding.

The outline of the exploration work is as follows:-

[A] The outline of the bottom sampling work



\* Detail of investigation (1)

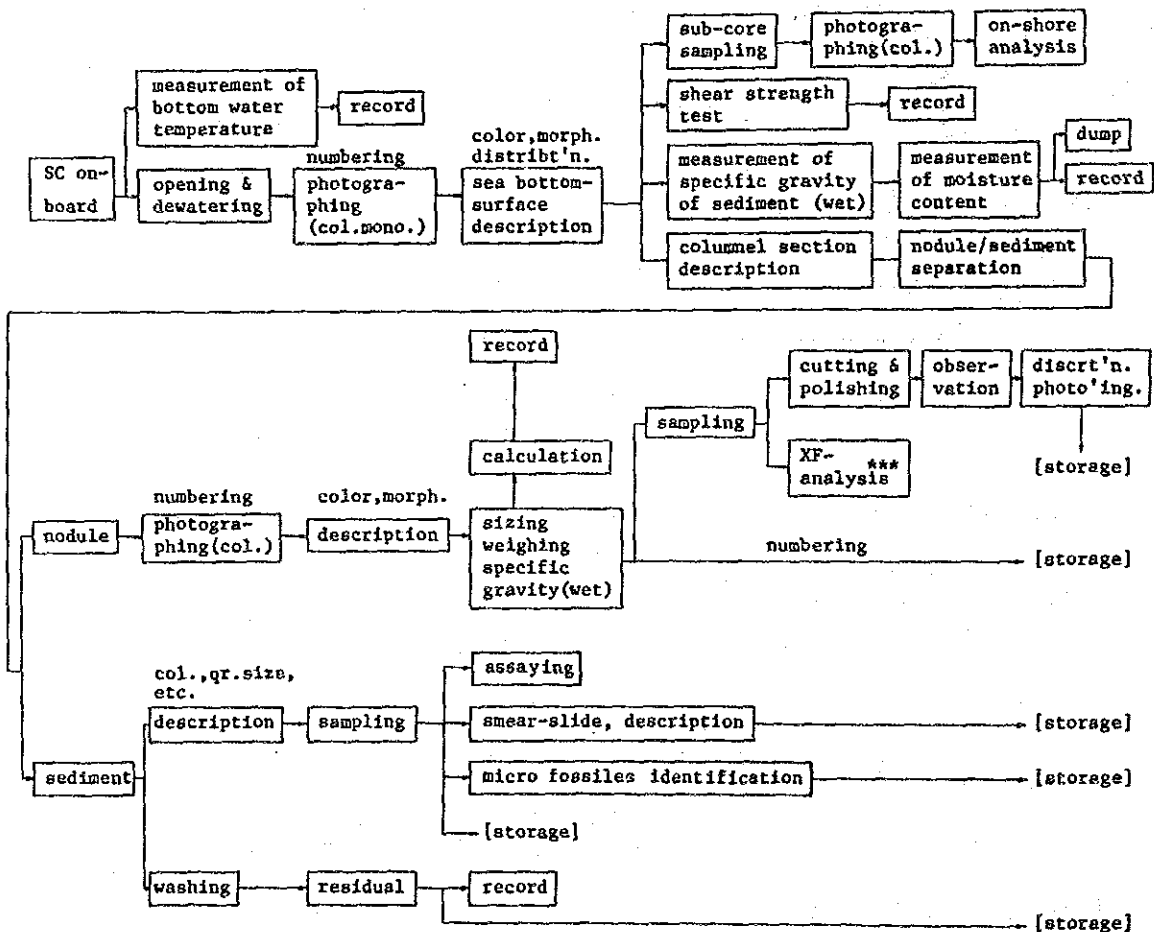
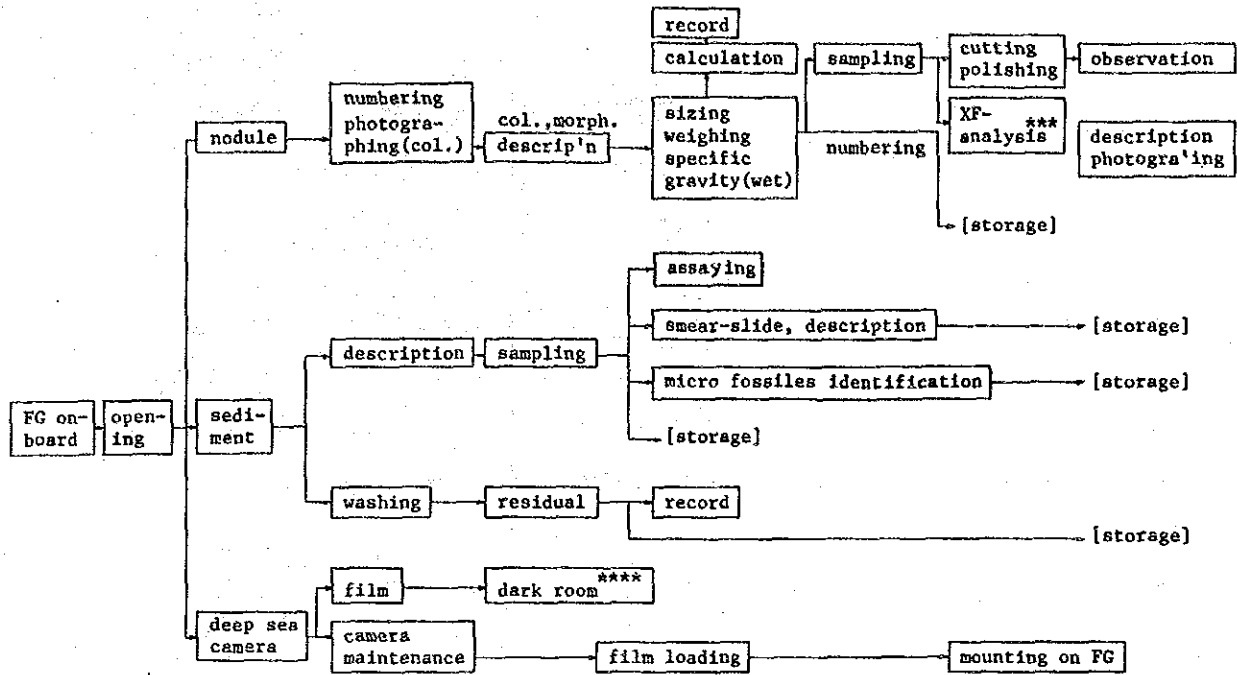


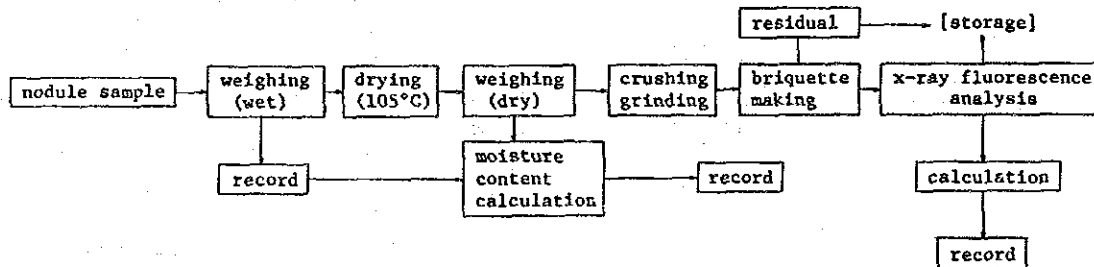
Fig. 3-7-1 Processing and Assaying Flowsheet of Samples (No. 1)



\*\* Detail of investigation (2)



\*\*\* Detail of XF-analysis



\*\*\*\* Detail of dark room work

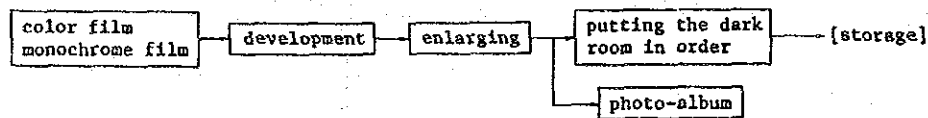
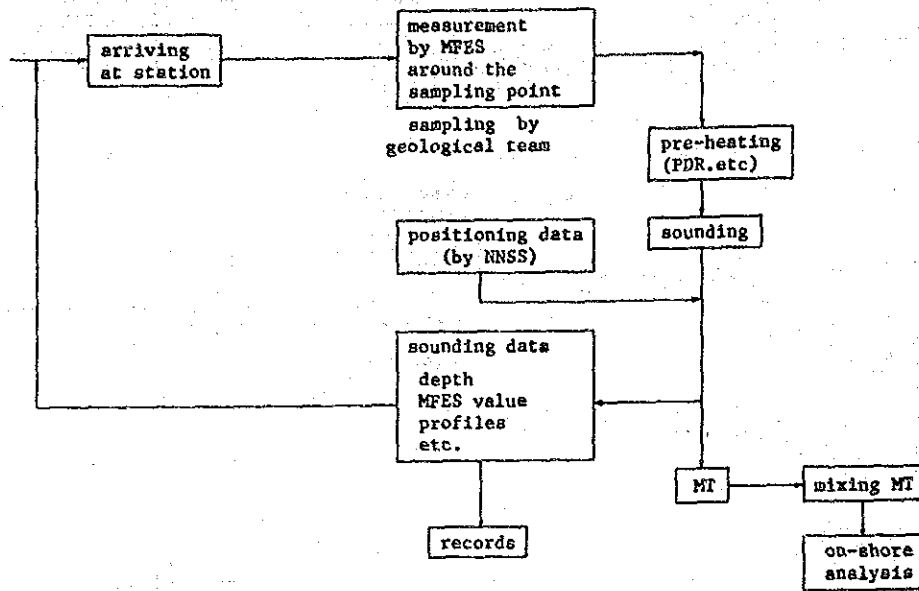


Fig. 3-7-1 Processing and Assaying Flowsheet of Samples (No. 2)

[B] The outline of the acoustic sounding



After surveying, on the way to the base harbor, all data are analyzed and evaluated. The outline of them are as follows:-

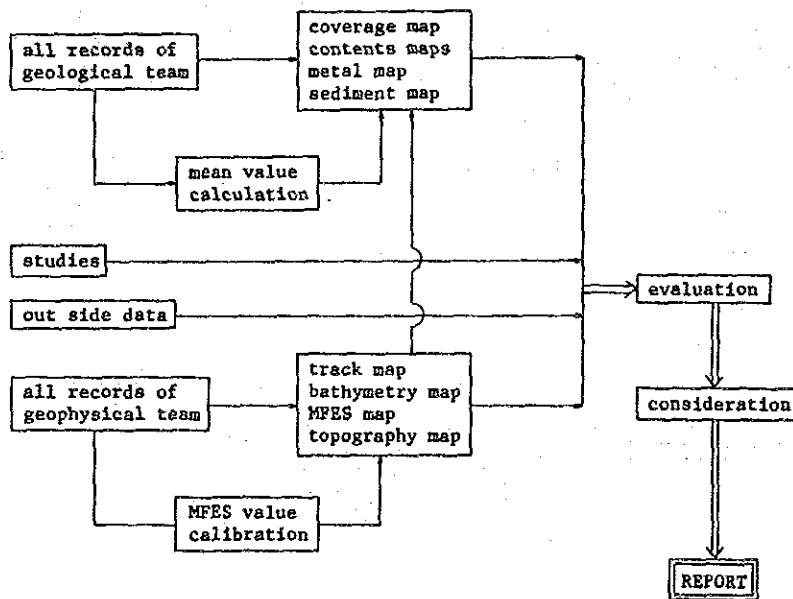


Fig. 3-7-2 Acoustic Sounding and Processing Flowsheet

### 3-8 Sea Bottom Observation by means of FDC

With a view to observe minutely the manganese nodules bearing on the deep ocean floor and the sea bottom situation, the sea bottom observation by means of FDC was carried out.

#### 1) Selection of the track lines for FDC

In selecting the observation lines for FDC within the sea areas of the present survey where the secondary sampling had been achieved, the fundamental conditions such as listed below were taken into consideration:

- (1) Possibility of observing the continuity of abundance of manganese nodules around the sampling stations where the abundance was highest.
- (2) The sea area where the embedding ratio of the manganese nodules was low would be suitable for analysis by photos.
- (3) There was no topographic limitation in the use of the FDC system which was practicable even in the area with a heavy sea floor undulation because of its photographing method which does not consist in taking successive photos by maintaining the FDC at a fixed level from the sea bottom, but in taking intermitent photos by landing the shutter sinker.

Moreover, the results of the secondary survey such as the sampling by FG, observation of the sea bottom by PDR and SBP, geological structure section of the sea bottom, measurement by MFES, were also taken into consideration to make a synthetic judgment. Finally, the two track lines with a total length of 90 nautical miles (effective length, 98 miles) were selected, as shown in Fig. 3-8-1.

#### 2) Interval of observation stations of FDC

The interval distance between the observation stations of FDC was fixed at 2.0 miles in all track lines, taking into consideration the continuity (in other words, variation) of manganese nodules abundance observed in last years' survey, the navigation method and the analysis method of surveyed results. Length and number of stations are given as follows.

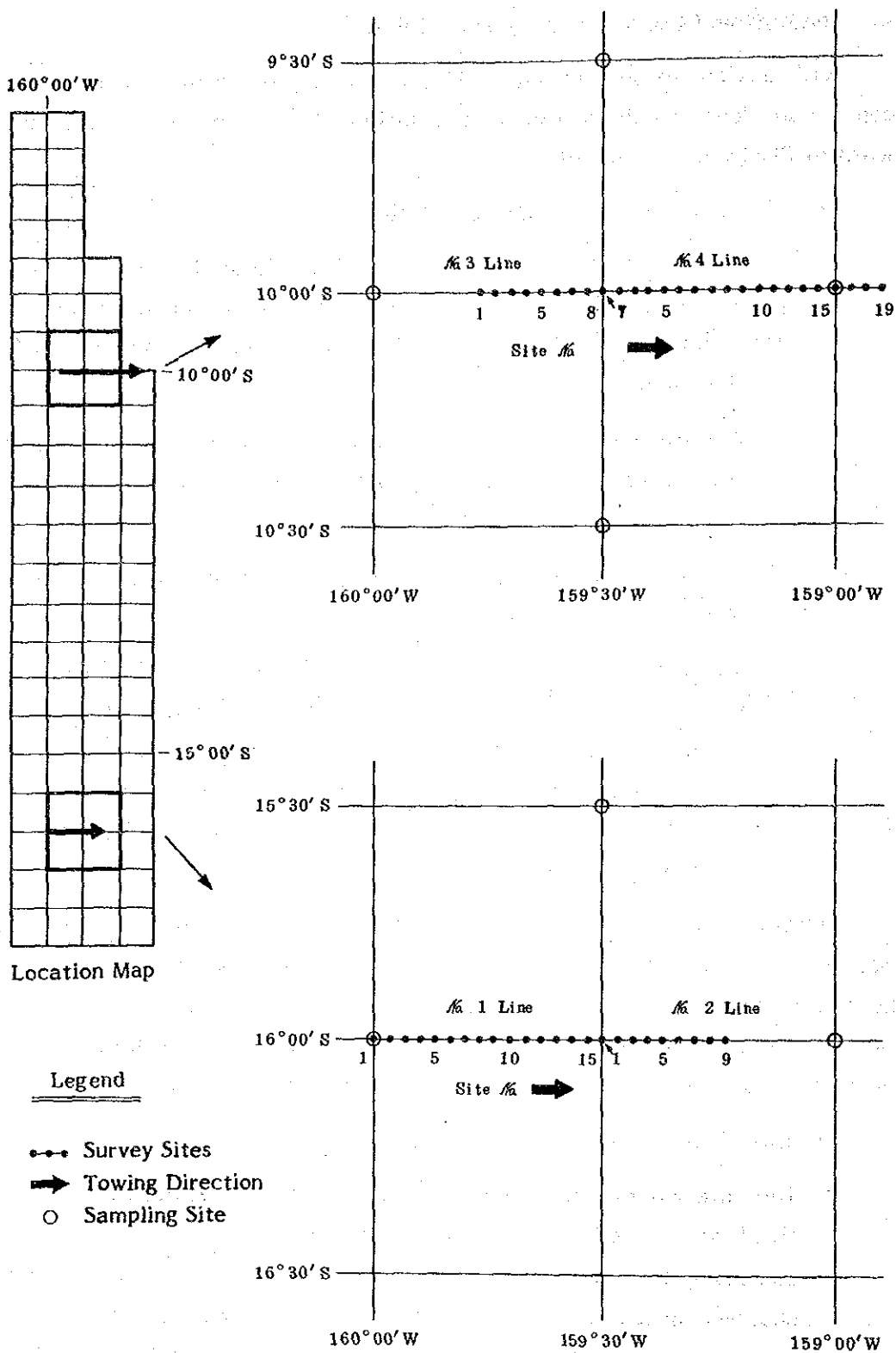


Fig. 3-8-1 Track Lines and Observation Stations of FDC-Survey

<u>track lines</u>	<u>designed length</u>	<u>effective length</u>	<u>effective stations</u>
No 1	30 miles	30.0 miles	15
No 2	15	16.0	9
No 3	15	16.0	8
No 4	30	36.0	19
total	90	98.0	51

As is shown in the above table, the total number of the observation stations is 51. Fig. 3-8-1 indicates the location of the observation stations.

3) Number of photos by FDC

5 photos were taken, in principle, in a observation station, but, in case of necessity, 4~12 photos were taken.

4) Photographing operation of FDC

From September 30 to October 1, observation was made at 24 stations on the 2 track lines, and from October 9 to October 10 at 27 stations on the 2 tracklines. 51 stations in total were observed. The abundance and the average size of manganese nodules were calculated by analyzing the 288 valid photos. The photography operation was carried out on the basis of the sea floor topography section established by the PDR. The standard of vessel speed is 1.0 knot/h at the time of sea floor observation.

5) Analysis of the photos by FDC

The covering surface ratio (COV) of the manganese nodules and their number (N) per  $1 \text{ m}^2$  were obtained by analyzing the sea bottom photos and the size of the shutter releasing sinker appearing in these photos. Using the following regression equation \*1, the abundance and the average granular diameter are calculated:

---

\*1 The regression equations were established to determine the coefficient on the basis of the abundance, the covering surface ratio and the number of the manganese nodules.

$$\text{Abundance (kg/m}^2\text{)} = 1.430 \times \text{COV}^{1.5}/\text{N}^{0.5}$$

$$\text{Average of diameter (cm)} = 16.62 \times (\text{COV}/\text{N})^{0.5}$$

These formulas were applied respectively to the 288 photos valid for photographic analysis.

The average of abundance and the average size at every station were obtained by arithmetic mean of the respective values of the analyzed photos taken on the concerned station.

In the case of the basement rock photos, its abundance value, which was assumed to be zero, was added to the number used in the calculation of the mean value of each station.

### 3-9 Processing and Analyzing of the Survey Data

Processing and analyzing of the survey data were carried out mainly on board, however, a part of data processing and synthetic analyzing was executed on shore.

#### 1) Survey data and its processing (cf. Fig. 3-7-2)

##### 1 Relating to cruising and acoustic sounding:

- o The vessel positions by NNSS (date, time, latitude, longitude) were printed out in the table of rectified vessel positions every minute from the data processing system on board.
- o The depth data by PDR (NBS) (date, time, values indicated in the digitizer and in the print-out papers) were registered in the field book every 5 minutes.
- o The superficial sediments by SBP (thickness of upper transparent layers, stratigraphy type) were registered in the field book every 5 minutes.
- o The values measured by MFES were registered in the field book every 5 minutes on the track lines between the sampling points and on the track lines between the observation points respectively.

##### 2 Relating to sampling:

The following survey data on manganese nodules, sediments, and assay etc., were registered in the field books for every sampling point.

- o Data relating to the manganese nodules: sampling amount, wet weight of each size, wet specific gravity, morphology, number, superficial structure, etc.
- o Data relating to the sediment: type of sediments, color tone, granular size, microfossil, etc.
- o Data relating to assay: grade of 5 principal components (Ni, Cu, Co, Mg, Fe) and water content.

- 3 Various photos:
  - o Sea bottom photos by deep-sea camera equipped on FC and SC, and by FDC, re-collecting photos, working photos.
  - o Record photos of physical prospection (PDR records, SBP records)

## 2) Analyzing of the survey data

The charts and tables essential for advancing the survey, were drawn up using the data available on board. These data were reanalyzed afterwards on shore in further detail. The results of the analyses are recaptulated in the following charts and tables.

### 1 Chart of track lines, location map of sampling points

The chart of track lines and the location map of sampling points were drawn up by plotting the positions on a 1/1,200,000 scale registering sheet based the table of recertified vessel positions printed out from the data processing system.

### 2 Map of sea floor topography

Using the sea depth chart obtained by plotting depth values of every 5 minutes on the above-mentioned track lines chart, the map of sea floor topography was drawn up with contour intervals of 200 m.

### 3 Thickness contour map of the upper transparent layers by SBP

Thickness of the upper transparent layers was read out every 5 minutes from the SBP record and plotted on the above-mentioned chart of track lines. Then the thickness contour map was completed with contour intervals of 10 m.

### 4 Distribution map of bottom materials

Distribution map of bottom materials was drawn by plotting types of bottom materials collected by the sampler and the quantity of authigenic minerals.



5 Abundance map of manganese nodules estimated by MFES

Abundance map of manganese nodules was accomplished by plotting the abundance (MEFS intensity) displayed every 10 minutes. Abundance contour lines was drawn up with the step of 10 kg/cm<sup>2</sup>.

6 Abundance map of manganese nodules, grade contour map, metal quantity map

On the basis of data obtained about the manganese nodules at each sampling point (setting down point of FG, SC, etc.), the average occurrence situation of minerals (values of abundance and grade etc.) was obtained for each station (3 samplings per one station). On the basis of these results, the abundance map of manganese nodules, the grade contour maps of nickel, copper, cobalt, manganese and iron and the metal quantity map of nickel, copper, and cobalt are drawn. The acoustic sounding data were also utilised in this process.

7 Table of the survey results

In order to facilitate searching and consulting the data on the manganese nodules obtained every day on board, the essential items \*1 were listed up from the field book to be captulated in the table.

8 Estimated abundance chart by FDC observation

Estimated abundance map by FDC observation was accomplished by plotting sampling data concerned and these calculated from coverage of manganese nodules on the FDC photos using the regression formula introduced by analyzing FG sampling data statistically.

---

\*1 The principal items are as follows:

latitude, longitude, sea depth, granular size distribution, values of abundance, morphology, grade, sediment, state of combination, etc.,

- 9 Observing the other relation between each of the elements such as bearing quantity of the manganese nodules, grade, morphology, bearing situation, topography, upper transparent layers' thickness, etc., studies have been carried out to define the potential field of manganese nodules.

## Chapter 4. Results of the Survey

### 4-1 Survey accomplishments

The surveying operations were accomplished as shown in Table 4-1-1.

Table 4-1-1 List of Survey Achievements

Item		Accomplishment	
Survey Schedule	Leaving the port of Honolulu	Sept. 05	16:00
	Arrival at survey areas	Sept. 11	02:00
	Leaving the survey areas	Oct. 13	07:00
	Entry to the port of Honolulu	Oct. 20	08:00
Accuracy (disposition of the stations)		Stations at the primary stage (42.4 miles grid) and Station at the secondary stage (21.2 miles grid)	
Sampling	Sampling stations	60 points sampling	total
	Sampling per one station	3 points	180
	Samplers used	Free fall samplers (176 samplings)	points
		Spade corers (4 samplings)	
	Failure due to non-floating	None	
Deep-sea camera	Use of deep sea camera	180 times	
	- successful cases	of which 174 times	
	- unsuccessful cases	6 times	
	due to	disorder in weight magnet	
		4 times	
		misfunction of frash valve	
		1 time	
		cut off wire of battery case	
		1 time	
Photo analyzing	Photo analyzing	162 cases	
	- analyzing of FG, SC photos	of which 174 cases	
	- analyzing of FDC photos	288 cases	

(Continue)

(Continue from previous page)

Item		Accomplishment				
Treatment						590 cases
		Ordinary samples				494 cases
		Extra ordinary samples				96 cases
Analyzed components		5 components; Ni, Cu, Co, Mn, Fe				
Total No. of analyzed components		582 cases x 5 components = 2,910 components				
Acoustic sounding	SBP	3.5 kHz	Distance of sounding surveyed = 4,187.4 miles			
	PPR	12.0 kHz	"			
	NBS	30.0 kHz	"			
	MFES		"			
	On line MT		10 reels			
	On line MIX MT		8			
	Sampling MT		2			
	Sampling MT MX		1			
	Atmospheric and marine meteorogy MT		2			
	Atmospheric and marine meteorogy MIX MT		1			
	(Total)		24 reels			
Name of track lines		86SFDC01	86SFDC02	86SFDC03	86SFDC04	total (average)
Total length of track lines (mile) (A)		30.0	16.0	16.0	36.0	98.0
No. of surveyed stations		15	9	8	19	51
Sea bottom observation by FDC	Required hours	28:59	12:18	13:18	27:39	82:41
	setting hours	06:01		01:56	01:35	09:32
	moving (T)	09:16	03:57	04:07	07:43	25:03
	preparation	08:04	05:31	06:16	12:48	32:39
	photographing	02:36	01:18	00:59	02:10	07:03
	re-collecting	03:02	01:32		03:23	07:57
	average speed (A/T) (knot)	3.24	4.05	3.89	4.67	3.91
	average minutes of photographing (min./pcs)	1.88	1.86	1.59	1.60	1.74
	Nb. of photos *	96	49	44	99	288

#### 4-2 Sea Floor Topography (cf. Annexed figure 2.

The present surveyed area is located at the western edge of the southern Penhryn Basin, to the east of the Manihiki plateau (relative height of 1,500 - 2,000 m), in the Central Pacific Ocean, and is north-south slender sea area which spreads over the zone of about 200 m east and west and about 1,200 km north and south. As for the general characteristics of the surveyed area, the sea floor topography shows variable types and in the north-south direction the area can be divided macroscopically into 4 provinces as follows.

- 1) Mountainous: the north-western part in the surveyed Area (western part of the channel existing to the north of 11°00'S)
- 2) Hilly: the north-eastern part in the surveyed Area (eastern part of the channel existing to the north of 11°00'S)
- 3) Plain: the central part of the surveyed area (spreading from 11°00'S to 15°00'S)
- 4) Quasi-Plain: the southern part of the surveyed area (southern part of 15°00'S)

The depth of surveyed area is generally between 5,100- 5,600 m except for the sea mounts and the sea knolls, as shown in the sea floor topography map (Fig. 4-2-1 and Fig. 4-2-2). As a general trend of the depth, the southern part is shallowest (5,000 - 5,100 m) and the depth increases gradually to the north and reads about 5,600 m at the northern end.

According to the microscopical classification of sea floor topography, shown in Table 4-1-1, followings were observed in the surveyed sea area: flats; hollows (includes ship-shaped basin); channel; platforms; sea knolls and sea mounts. Flats spread widely over the central part and the south part in surveyed area. Hollows and ship-shaped basins are distributed spottedly over the whole surveyed area, and especially abound in quasi-plain existing to the south of 15°00'S line. Its general direction of disposition is slightly north-south. The channel spreads north and south on the 159°40'W line approximately, in the north part of the surveyed area (north to the 11°00'S line). It is only 5 to 10 miles in width but spreads over 240 miles continuously in length. The average depth of the channel is 5,600 m (6,700 m at the deepest point). It can be considered that

Table 4-2-1 Classification of Sea Floor Topography

Topographical classification		Definition
Regional province	Plain	Area whose bottom is almost flat and even with a isolated sea mount or sea knoll, it may be considered as plain from a general point of view;
	Hilly	Area where numerous sea hills or sea mounts are dispersed;
	Mountainous	Area where a group of sea mounts are located;
	Quasi- plain	Area where the outstanding mounts or hills are scarcely observed but the bottom is rather undulated and which is classified neither as plain nor as hilly.
Local area	Flat	Plain area not undulated or smoothly undulated (up to about 100 m relative height) and which doesn't belong to neither the hollow nor the platform.
	Hollow	Area with smooth undulation and which presents a generally concave terrain, including a ship- shaped basin.
	Channel	Long and narrow concave terrain in a ditch shape, including fissures or fracture zones.
	Platform	Area with smooth undulation which presents as a whole a convex terrain (or a tableland)
	Sea Knoll	Hilly area with a relative height of more than about 1,000 m, including entire slop as well as summit
	Sea mount	Hilly area with a relative height of less than about 1,000 m, including entire slop as well as summit (the sloping surface contains a shifting part of the plain)
	Ridge	Terrain presenting a chain of mountain composed of the sea knolls and hills ranged in a zone.
	Other	Terrain not belonging to any of the above-mentioned classifications.

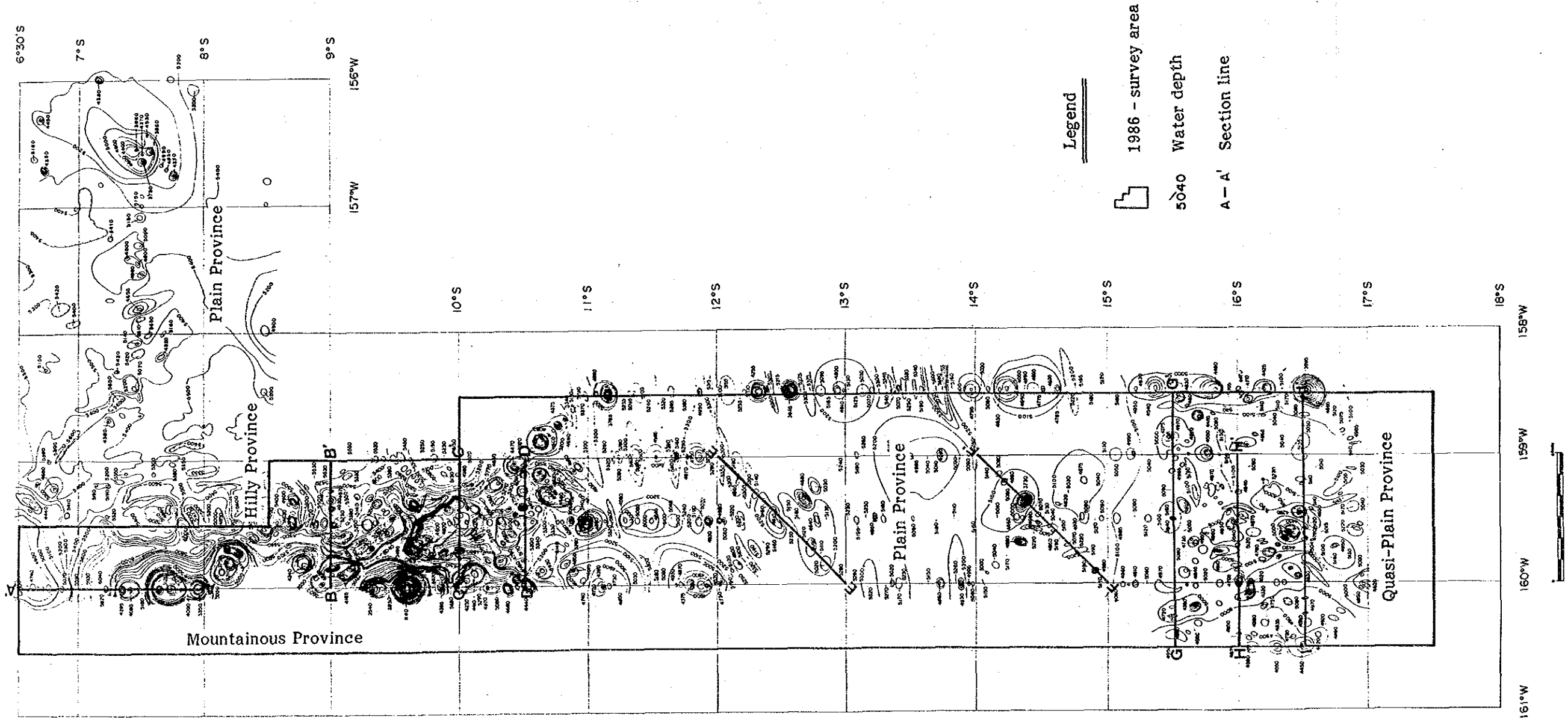


Fig. 4-2-1 Explanation of Sea Floor Topography

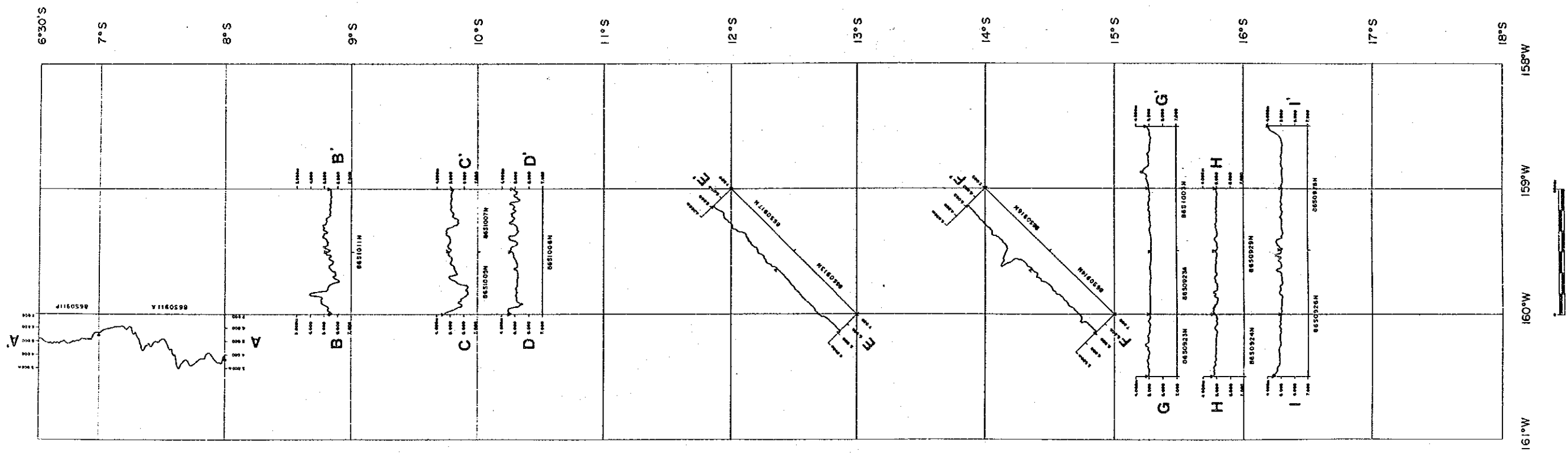


Fig. 4-2-2 Section of Sea Floor Topography





this channel should be a part of the eastern sinking edge of the Manihiki plateau which is spreading widely to the west of the surveyed area. The platforms are distributed mainly in the central and southern parts of the surveyed area where the plain and the quasi-plain are predominant. Its relative height is between around 100 - 200 m.

Sea knolls are distributed massively in the hilly province which is spreading to the east of the channel and existing to the north of the 11°00'S line. It should be noticed that sea knolls stand in a line along the channel. As for the relative heights, many sea knolls indicate between 300 m - 800 m (water depths 4,100 - 4,800 m).

Sea mounts are distributed in the mountainous province spreading to the west of the channel existing to the north of the 11°00'S line. They are disposed in the north-south direction which coincides with the elongation direction of the channel. Several mounts with relative height of between 1,100 - 1,800 m (water depths: between 1,860 - 4,255 m), are observed even in the plain province and quasi-plain province.

#### 4-3 Superficial Sediment

##### 1) Classification of SBP records

SBP records are classified into 9 types: type a, type b, type bc, type c, type d, type d2, type ds, type cl and type ts based on its reflective patterns.

In the present survey, the ac type is added to the above-mentioned 9 types. This type has an intermediate nature between type a and type c.

Definitions and characteristics of each type are as follows.

- 1 Type for which the acoustic transparent layers are recognized at their upper part (cf. Fig. 4-3-1-(1))

Type a: presenting a double layer structure of transparent and opaque, the transparency of the transparent layer is high (faded out completely) and the boundary with the opaque layer is relatively clear; the thickness of the transparent layer measures 10 - 50 m;

Type b: similar to type a, composed of two layers such as transparent and opaque, but the transparency of semi-transparent layer is not so high as to be called completely transparent. The thickness of transparent layers measures 30 - 100 m and generally speaking it is not a rare case that the thickness could be more than 50 m; the thickness varies markedly as compared with other type.

Type e1: presenting the multistratified structure of transparent and opaque layers; the clearly stripe thin opaque layer is recognized directly beneath the upper transparent layer. The thickness of the transparent layer including that of the striped opaque layer is generally 10 - 40 m.

- 2 Types for which the acoustic transparent layers are not recognized at their upper part (cf. Fig. 4-3-1-(2)).

Type c: the type composed of 3 layers: opaque, transparent and opaque: though it was not confirmed on the print-out papers, it is presumed that an external thin transparent layer could be found at the top of the upper transparent layers.

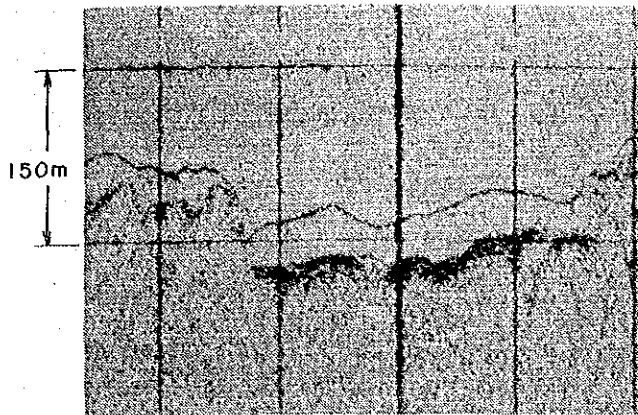
Type d1: Composed only of opaque layers. Generally, this type is found at sea mounts, sea knolls, etc., and these sites correspond approximately to their exposed basement rocks.

Type d<sub>2</sub>: similar to type d1, it is composed only of opaque layers; this type is observed mainly in plains and these sites correspond approximately to basement rocks or coarser grained sediments.

- 3 Other (cf. Fig. 4-3-1-(3))

type ts: it may be presumably composed of transparent and opaque layers; for this type, the records are not clear because of the dispersion of sounding waves by the undulated floor.

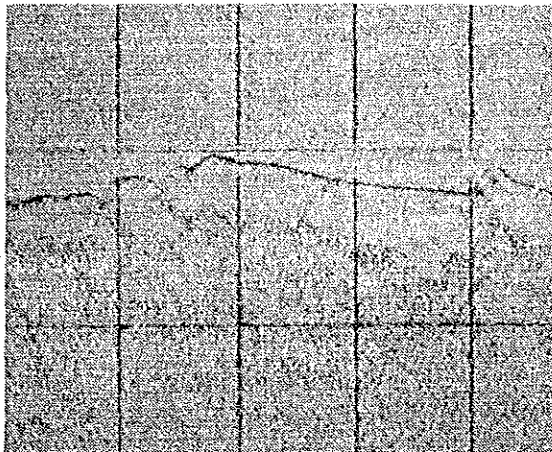
Type bc: basically, it may be composed of 2 layers: transparent and opaque, similar to type b; the bottom surface of the top superficial layer indicating a transparent layer does not form one line but always contains some noise, and further the transparency



Type a

Line No. 86S0926N

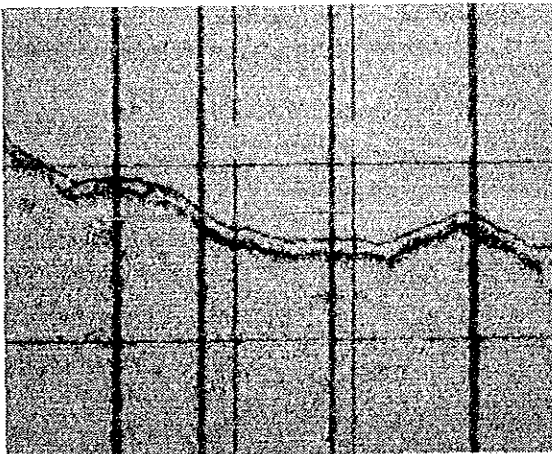
16°40.9' S : 160°19.3'W



Type b

Line No. 86S0922A

13°44.5' S : 159°29.9'W

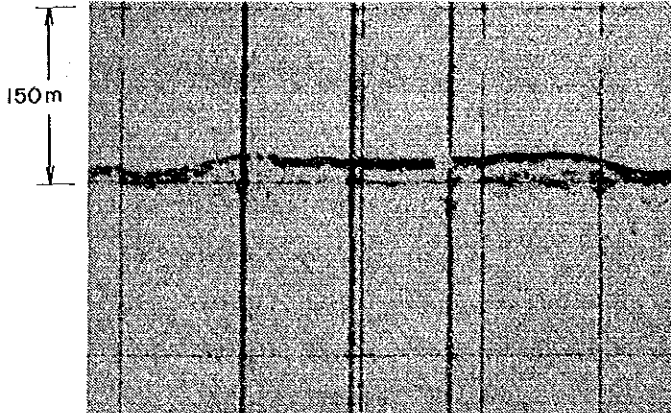


Type ei

Line No. 86SI006B

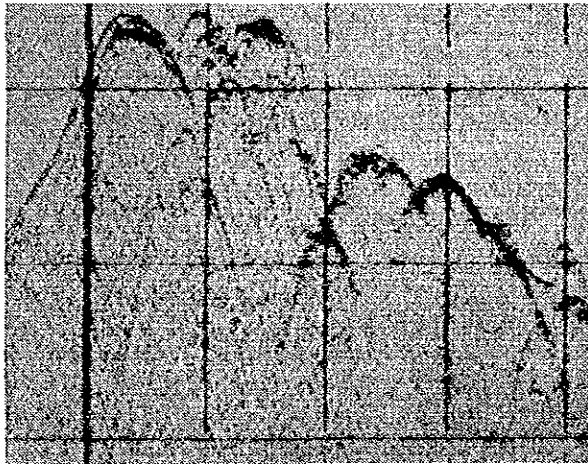
10°44.0' S : 159°16.0'W

Fig. 4-3-1-(1) Classification of SBP Records



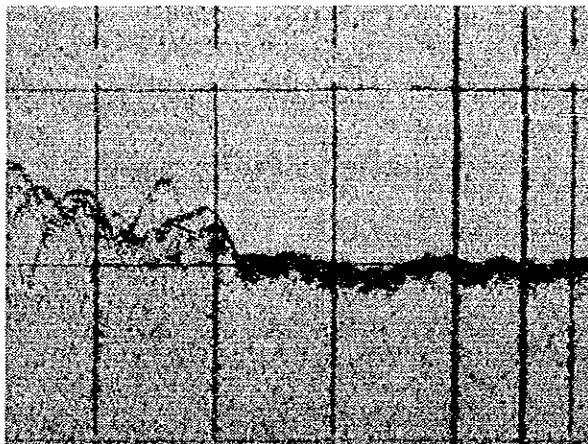
Type c

Line No. 86SI011N  
 09°00.1' S : 159°01.7' W



Type d1

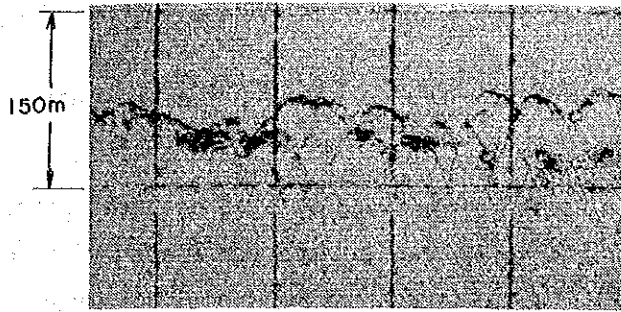
Line No. 86SI012N  
 09°57.2' S : 159°32.7' W



Type d2

Line No. 86S0923N  
 15°29.9' S : 160°29.3' W

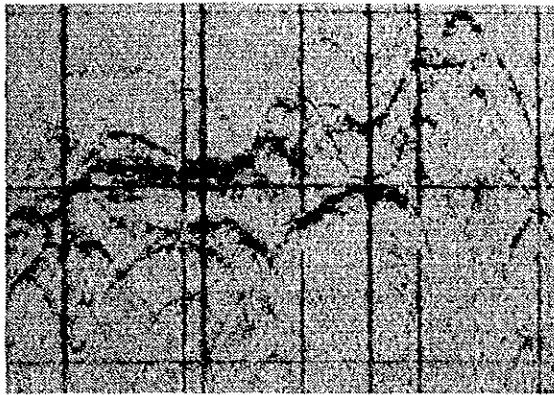
Fig. 4-3-1-(2) Classification of SBP Records



Type ts

Line No. 86S0923N

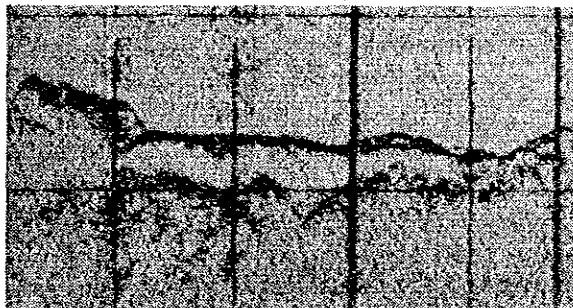
15° 57.0' S : 160° 02.6' W



Type ds

Line No. 86S1012A

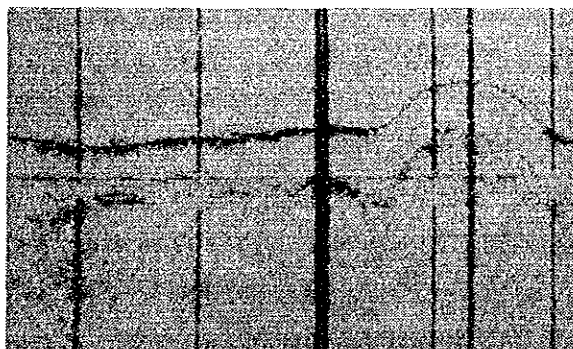
09° 29.9' S : 158° 59.6' W



Type bc

Line No. 86S0926N

16° 17.1' S : 159° 17.3' W



Type ac

Line No. 86S0925P

16° 30.2' S : 159° 59.8' W

Fig. 4-3-1-(3) Classification of SBP Records

(better than that of the above type bc) is unstable and partially presents the opacity.

Type ac: basically, it may be composed of 2 layers: transparent and opaque, similar to type a; the bottom surface of the top superficial layer indicating a transparent layer does not form one line but contains some noise, and further the transparency (more transparent than that of the above type bc) is unstable and partially presents opacity (opaque layer)).

## 2) Distribution of SBP types (cf. Annexed figure 4)

In the northern part of the surveyed area, it is recognized that predominant features of sea floor macroscopically are mountainous and hilly. Reflecting these features, in the SBP records, is observed mainly in the type lacking superficial transparent layer, disposition of which shows north-south direction.

From the central part to the southern of the surveyed area, no remarkable directional disposition is observed on the SBP records because the areas are far from Manihiki plateau and consequently independent of its geographic influence.

Moreover, types having transparent layer in the upper part become predominant ones in the SBP record classification.

The distribution of each type of SBP records is generally concordant to the water depth or sea floor.

### 1 North-west part of the surveyed area

In the western area of  $159^{\circ}40'W$  line, sea mounts having relative height between 1,100 - 2,680 m lie in a north-south row, along which type dl is widely extended.

### 2 North-east part of the surveyed area

In the eastern area of  $159^{\circ}40'W$  line where of sea floor is hilly, sea knolls with the relative height between 300 - 800 m are distributed along the channel, and type ds corresponding to this situation features shows almost the same distribution.

Type  $d_1$  is distributed in the topographic high and sea knolls. On the other hand, type c is distributed in the concave terrain called hollow area (ex; the point around  $9^{\circ}00'S$ ,  $150^{\circ}00'W$ , sea depth of 5,500 m). On the platform or the flat top of sea mounts, a transparent layer may be recognized locally though thickness of which is thin.

3 The central part of the surveyed area

The area from  $11^{\circ}S$  line to  $15^{\circ}S$  line is classified into a plain province, where type bc is distributed in almost whole area, while type  $d_1$  is observed on the scattered sea mounts in the area. And type  $e_1$  is distributed in the area shifting gradually between type ds and type bc. The thickness of the upper transparent layer of type  $e_1$  is as thin as about 10 m at most. Type a is distributed in the flat part of the transitional zone from hilly to plain. The thickness of the upper transparent layer shows between 20 - 30 m.

4 The southern part of the surveyed area

In the southern area of  $15^{\circ}00'S$  line, the predominant feature of sea floor is quasisi-plain. Type  $d_1$  distributed corresponds to the distribution of the sea knolls. Whereas type a and type bc are widely distributed in flat areas, type ac is recognized in the transitional part from type a to type bc.

3) Thickness and its distribution of the thickness of upper transparent layer in SBP profiles (cf. Annexed figure 5).

The distribution situation of the thickness of upper transparent layer is nearly corresponding to that of the types of the SBP record.

Observing the thickness of upper transparent layer by respective SBP type, for type a, thickness measures 10 - 40 m; for type b, 50 - 70 m; for type bc, 10 - 60 m; for type  $e_1$ , 5 - 15 m; for type ac, 10 - 60 m; while for type c,  $d_1$ ,  $d_2$  and ds, transparent layer was not recognized.



#### 4-4 Research on Manganese Nodules by means of MFES

##### 1) Factors affecting MFES

###### (1) Size of manganese nodules (weight coefficient)

By means of MFES, the sound magnitudes of three different frequencies such as NBS (30 KHz), PDR (12 KHz) and SBP (3.5 KHz), were measured individually and summed numerically to the compound sound pressure so as to estimate the abundance of manganese nodules on the deep ocean sea floor. Supposing a linear relation between the compound sound pressure and the abundance of manganese nodules  $V$  ( $\text{kg}/\text{m}^2$ ), a hypothetical formula listed below was given a priori. Later parameters  $a$  and  $b$  were determined based on the field data;

$$V = a Rt + b,$$

According to the supposition by means of MFES, the compound sound pressure ( $Rt$ ) is in proportion to the covering ratio of bottom surface, regardless of the granular diameter of manganese nodules.

Therefore, MFES detects the covering ratio of manganese nodules first based on the compound sound pressure which is reflected by the surface of manganese nodules and then the abundance of manganese nodules are calculated with weight coefficient given independently which means weight per unit covering surface of manganese nodules.

$22 \text{ kg}/\text{m}^2$ \*<sup>2</sup> was the weight coefficient\*<sup>1</sup> of manganese nodules adopted tentatively through the survey for immediate data analysis.

As is shown in Fig. 4-4-1, there were many observation points which showed a weight coefficient value more than  $40 \text{ kg}/\text{m}^2$  in the surveyed area and the actual average weight coefficient of the

whole area was 36 kg/m<sup>2</sup>. This indicates that the granular size<sup>\*3</sup> of manganese nodules in the survey area is larger than the gradular size estimated by means of MFES<sup>\*2</sup>. In other expression, the diameter<sup>\*3</sup> obtained by MFES were underestimated in comparison with the real diameter. Therefore, the weight coefficient was needed to be adjusted in order to obtain more accurate abundance of manganese nodules by following formula:

$$\begin{aligned} &\text{The estimated abundance by MFES (kg/m}^2\text{)} \\ &= \text{tentative abundance} \times \text{Weight coefficient} \\ &\quad \text{(fixed afterwords)/22 ..... (2)} \end{aligned}$$

(2) Topography and bottom materials

The relation between the estimated abundance (MFES Intensity) of manganese nodules obtained by MFES observation and the abundance by sampling in the survey area is shown in Fig. 4-4-2-(1). Each station is indicated by SBP type in this figure. As shown in Fig. 4-4-2-(1), type d<sub>1</sub> which indicates sea mounts and sea knolls, worsens the correlation. This suggests that strong scattering wave or side-echo may cause the disturbance of measurement where sea mounts and sea knoll are predominant, and that NBS nad PDR waves cannot follow a sudden change in sea depth. The relation between MFES Intensity and abundance obtained by sampling is

\*1 Weight coefficient (kg/m<sup>2</sup>) =

$$\begin{aligned} &\text{Recollected weight of manganese nodules (kg)/} \\ &\quad \text{(covering surface ratio X Grab-opening area (m}^2\text{))} \\ &= \text{Abundance of manganese nodules (kg)/} \\ &\quad \text{Covering surface ratio} \end{aligned}$$

\*2 This was used to determine the parameter of the formula (1)

\*3 Although other factors such as shape exercise influence, this can be considered as the influence of granular size as most manganese nodules bearing in the surveyed area are spheroidal.

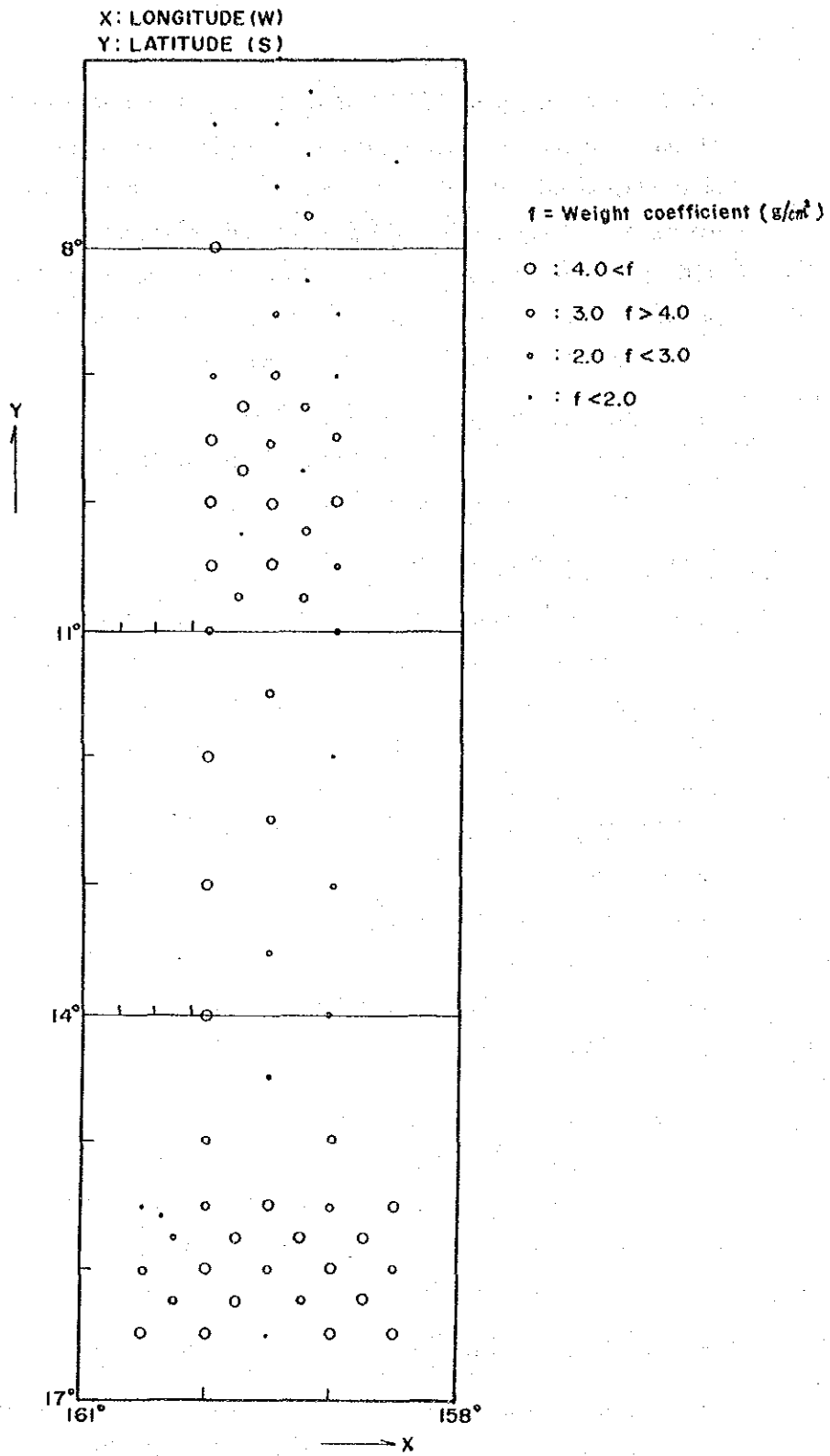


Fig. 4-4-1 Distribution of Weight Coefficient

shown in Fig. 4-4-2-(2) excluding points of sea mounts and sea knolls. As shown in Fig. 4-4-2(2), the correlation coefficient indicates a better value of 0.83, but this is not still sufficient. It seems that the possible elements of this disturbance may be the stations such opaque layers as type  $d_2$  and  $d_s$ .

The main reasons why normal value cannot be obtained is as follows;

- o Sound cannot reflect normally, therefore, catoptric wave shows scattering wave or sound-echo
- o Sound pressure reflected by rock or hard bottom materials tends to be higher than that reflected by the normal sea bottom where manganese nodules are abundant.

The relation between MFES Intensity and abundance obtained by sampling is shown in Fig. 4-4-2-(3) excluding points of types  $d_1$ ,  $d_2$  and  $d_s$  composed of only opaque layer. As shown in this figure, the correlation coefficient shows more than 0.9, a good correlation. The characteristics of surveyed areas, as is evident in Fig. 4-3-2 and Annexed figure 6, is that the observation stations distributed in the limits of type c area are estimated to constitute a sterile zone while the stations in the limits of type a area are estimated to constitute a high abundance zone of manganese nodules.

In analyzing the abundance of manganese nodules in the area where SBP type indicates only opaque layer, it is necessary to take into consideration that normal sound pressure was rarely obtained. Specially at the area where the opaque layer covers a great portion of the whole sea area, like this survey area, it is highly probable that Quasi-anomalies such as high abundance areas can be constituted where types  $d_1$ ,  $d_2$  and  $d_s$  are distributed.

### (3) Embedded manganese nodules

The distribution of embedded manganese nodules in the survey area is shown in Fig. 4-4-3. Most of manganese nodules in the survey area are the exposed type.

The embedded type\*<sup>1</sup> appears in the northern part generally, and typically in the northern most part contiguous to the area surveyed last year.

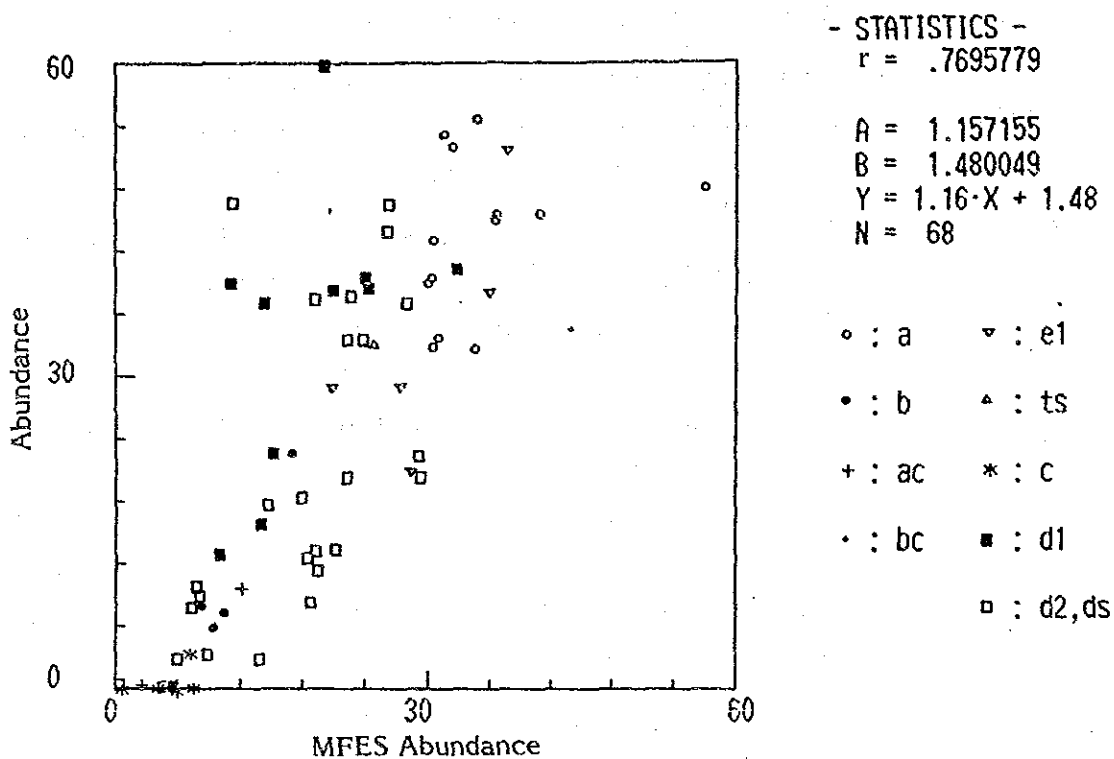
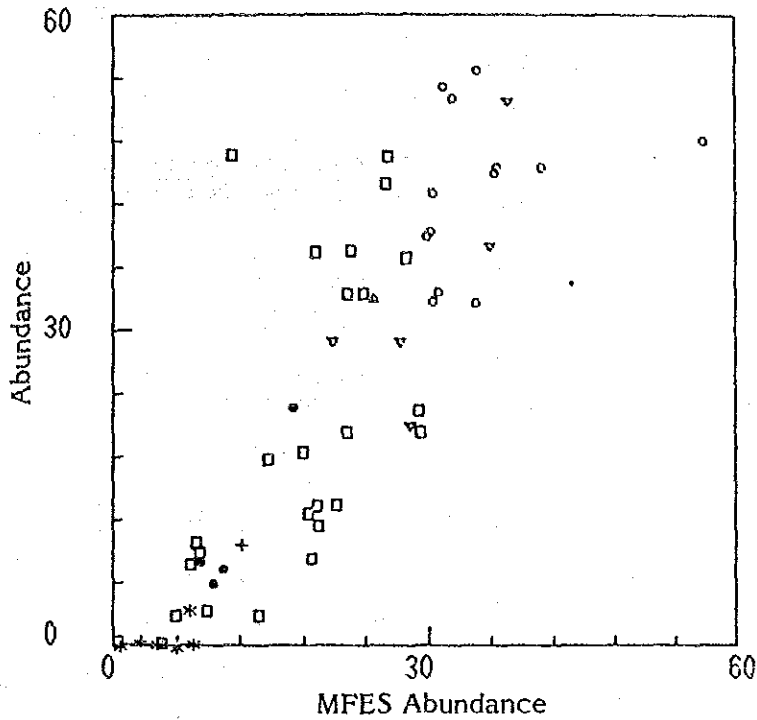


Fig. 4-4-2 Relation Between MFES Intensity and Abundance of Manganese Nodules

\*1 The degree of manganese nodules embedded is considered high in such case as;  $1 - (\text{coverage by deep-sea camera} / \text{coverage by samples obtained}) = 0.4$



- STATISTICS -

$$r = .8335671$$

$$A = 1.186292$$

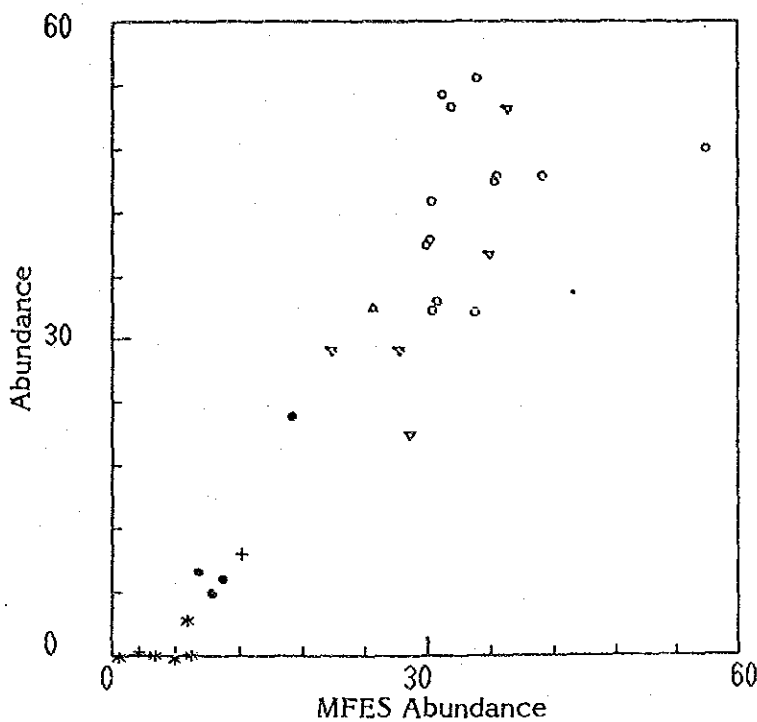
$$B = -1.097214$$

$$Y = 1.19 \cdot X - 1.10$$

$$N = 57$$

- o : a      ▽ : e1
- : b      ▲ : ts
- + : ac     \* : c
- : bc     □ : d2,ds

Fig. 4-4-2 Relation Between MFES Intensity and Abundance of Manganese Nodules



- STATISTICS -

$$r = .9026544$$

$$A = 1.197909$$

$$B = -1.714887$$

$$Y = 1.20 \cdot X - 1.71$$

$$N = 31$$

- o : a      ▽ : e1
- : b      ▲ : ts
- + : ac     \* : c
- : bc

Fig. 4-4-2 Relation Between MFES Intensity and Abundance of Manganese Nodules

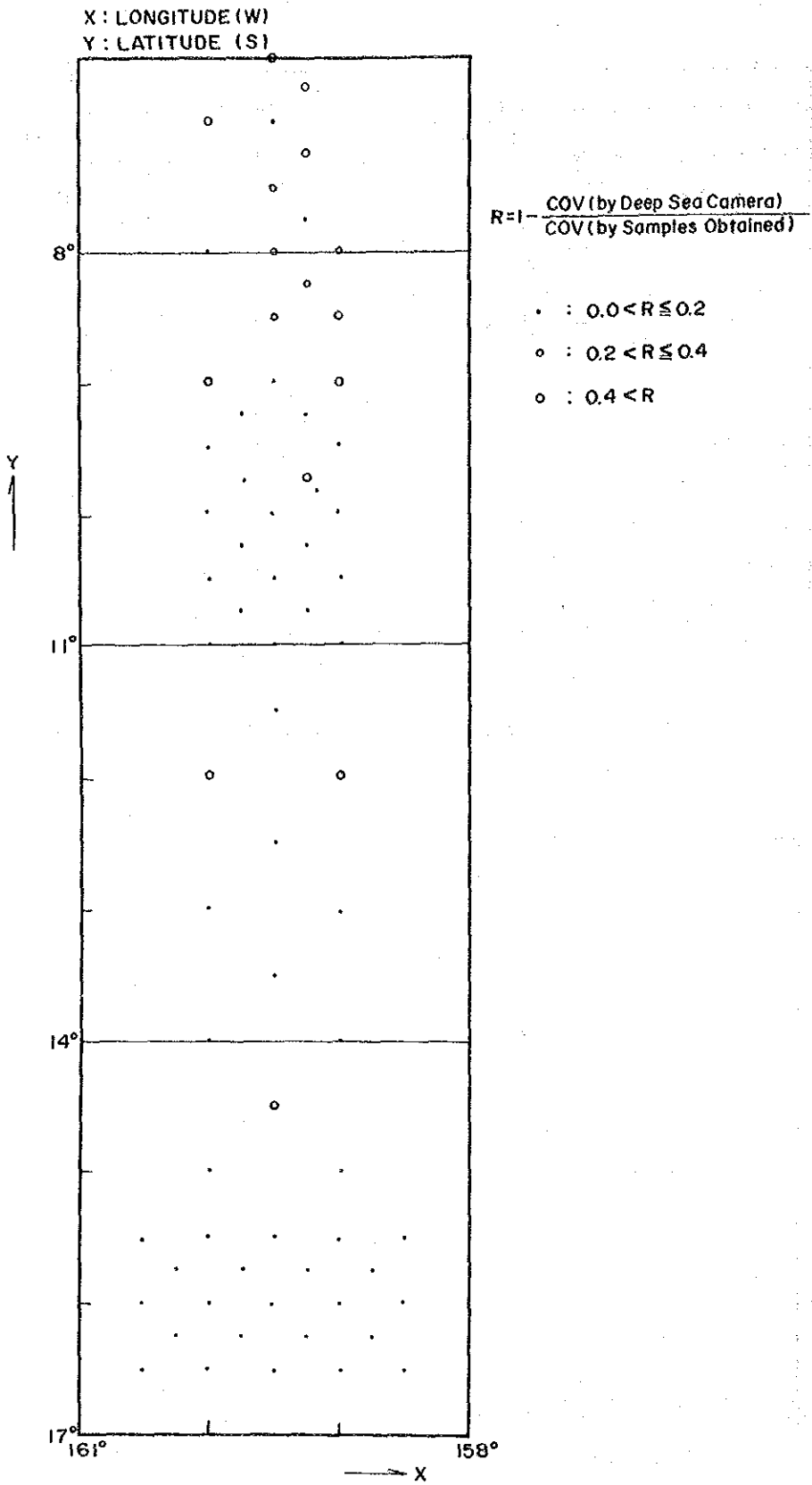


Fig. 4-4-3 Distribution of Embedded Type Manganese Nodules

Although it was already pointed out that the embedded manganese nodules were able to be detected by MFES, its reexamination was done again. The result is shown in Fig. 4-4-4. The stations of highly embedded manganese nodules are represented by black circles.

As shown in this figure, although the abundance of embedded manganese nodules is very low, it is apparent that MFES detects these fairly well. In spite of low MFES Intensity, the embedded type still coincides with the regression line.

## 2) Estimation of manganese nodules by means of MFES

The estimated abundance of manganese nodules by means of MFES is shown in Annexed figure 6. Data processing is described in proceeding paragraph.

The figure shows that the abundance of manganese nodules in this survey sea area is quite high.

The main characteristics of high abundance zone in connection with sea floor topography and types of SBP record are described as follows;

### 1 The mountains and hills (north of the $11^{\circ}\text{S}$ ; northern part of the survey area)

Predominant are sea mounts, sea knolles and channels in most cases, and also SBP type  $d_1$  and type  $ds$ . In this area, the measuring condition of MFES is worse because of scattering wave and sound-echo, therefore it is to be estimated that the reliability of the estimated abundance of manganese nodules is low. It is necessary to be careful in analyzing the abundance in such a sea area.

The areas with upper opaque layer that have high possibility of a quasi-anomaly are represented by horizontal lines so that they can be distinguished from others.



2 The plains (11°S - 15°S; central part in the survey area)

This is the area where sea floor topography is flat, and where SBP classification shows predominantly types having upper transparent layer are predominant, and where the reliability of MFES is relatively high.

This area indicates over 10 kg/m<sup>2</sup> of abundance throughout the area. Especially there are two sites where the abundance is more than 30 kg/m<sup>2</sup>, namely the sites around the position 12°30'S:159°W and 13°30'S:159°W.

3 The quasi-plains (south to 15°S; southern part of the survey area)

This is the area whose bottom is almost flat with scattering sea mounts and sea knolls. SBP type a was also recognized between sea mount and sea knoll. It can be said that the area consists generally of a broad continuous zone with dense distribution of manganese nodules detected more than 30 kg/m<sup>2</sup> by MFES

Especially the abundance is more than 60 kg/m<sup>2</sup> at the sites around the positions 16°20'S:159°50'W and 16°30'S:160°30'W. It is to be estimated that this appears a rather great amount of manganese nodules judging from the great extent and the stable abundance. Therefore, the area appears the most promising in the survey area because of the flat sea floor and the abundance.

On the other hand, it is highly probable that the area where SBP type d<sub>2</sub> is distributed around sea mounts and sea knolls is an false anomaly area. In this figure, this area is represented by horizontal lines so that it is distinguished from others.

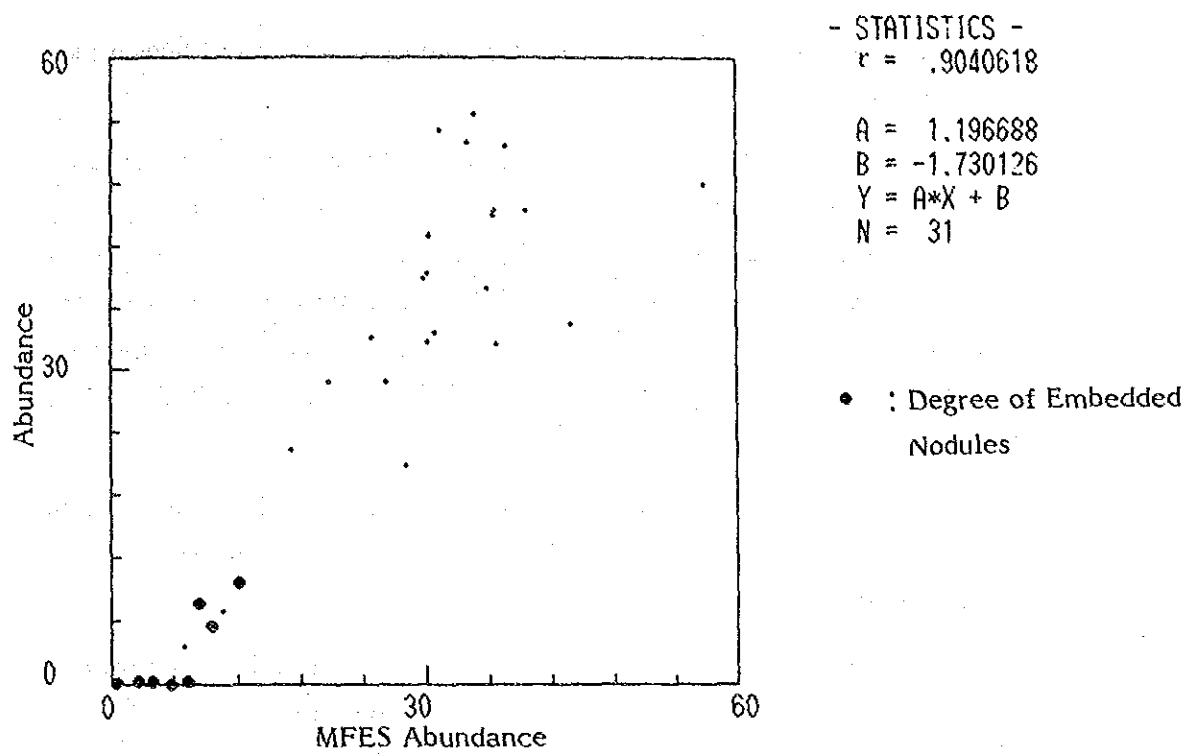


Fig. 4-4-4 Influence of Embedded Type Manganese Nodules on MFES Measurement